

Author response to reviewer comments

acp-2016-98

‘Chemical and isotopic composition of secondary organic aerosol generated by α -pinene ozonolysis’

Carl Meusinger, et al.

I checked the revised manuscript. The authors responded to our comments in professional manner, and attempted to reorganize the manuscript along the comments. *Thank you.*

It is intriguing to see what products the ozonolysis of alpha-pinene produces and how carbon isotopes are balanced between the gas-phase and condensed phase products.

We agree.

Furthermore, application of PSIA to reaction mechanism study seems to have potential to fingerprint its products in general. After reading the manuscript carefully, however, it was found that the corrections and modifications were not satisfactory and the manuscript has writing issues that need to be solved. Overall, the manuscript still needs substantial revision. The followings are some examples of writing issues I encountered.

There were many sentences that it was hard to understand. For example, in the sentence in P4L29, “If...”, I didn’t know what “depletion of the gasphase” means, and I didn’t get the logic why depletion of ^{13}C at C9 position leads to it.

We have rewritten the passage to be more clear:

‘It is widely understood that the enrichment/depletion of a product depends on the enrichment of the starting material, the isotopic fractionation occurring in the mechanism of its formation, and the extent of reaction. Using PSIA we can take this analysis one step further: the enrichment of a product will depend on the position-dependent enrichments of the atoms from which it is formed. For example the ozonolysis mechanism transfers the C9-atom in α -pinene into several small, volatile products (see blue squares in Fig. 1). If the C9-position was depleted in ^{13}C the gas phase products containing this atom would be depleted, and the SOA correspondingly enriched, if the position dependent effect was stronger than kinetic isotope effects.’

For the sentence in P7L26, I could not understand what kind of correction the authors have made. The authors should make a message in every sentence clear as writing.

This passage describes the process of assigning chemical formulas and controlling / checking the assigned chemical formulas. No ‘correction’ was described or made in this passage. We are sorry to say that we are not sure how to rewrite the passage to improve clarity.

There were also unnecessary sentences and paragraphs (I was impressed that those were unnecessary, but those may turn to be valuable, depending on for what the authors are going to explain using those sentences and paragraphs). For example, a paragraph in P3L9-18 defines a KIE and an epsilon value. However, any KIE and epsilon value for the pinene reaction never came out in the text. Those definitions may not be necessary, if the authors are not going to use the KIE in the interpretation.

The passage in question was completely rewritten:

‘Isotopic substitution can cause reactions to be faster or slower than for the

unsubstituted case, kinetically fractionating the isotopes and leading to isotopic enrichment or depletion in the products. This is known as the kinetic isotope effect (KIE). If a reaction leads to a single product, the product may initially have a different abundance, but due to the law of mass balance will achieve the same abundance as the reagent as the reaction goes to completion. If a reaction has multiple product channels, enrichment or depletion will occur if there are isotope dependent changes in the product branching ratios.'

It is also not clear how the authors are going to discuss the observed isotope fractionation with functionalization, fragmentation, and oligomerization introduced in P3L27-P4L15. This paragraph impressed me at the beginning that the authors would discuss isotope fractionation at these reactions later to interpret the own data, but actually those were not discussed. If those are not available from own data or references, statements for combinational use of “isotope” and “functionalization (or oligomerization, fragmentation)” using one or two paragraphs may want to be avoided. Many of these things were piled up, and, at the end, I was not sure what I gained by reading the manuscript.

We disagree. These terms are used extensively throughout the manuscript in discussing the origin of the observed results. In fact we refer back to these terms many times, be it when discussing O:C ratios or the isotope effects. We have revised the conclusions to be sure that we resolve questions raised earlier in the manuscript.

The way to refer Supplementary Information, Tables, and Figures, also needs to be checked with the author's guide.

Thank you, we have checked that our usage is consistent with the preparation guidelines. Specifically, the term 'in the SI' was omitted throughout the manuscript.

Many figure captions and table headings also included unnecessary description, which can be inserted in the text.

We have revised the figure captions and table headings in line with the preparation guidelines. However, please note that the author's guide asks for concise but descriptive captions. We tried our best to delete unnecessary content from the captions. In case abbreviations were included in the captions, doubles were deleted if they were introduced in the text before.

For these reasons, I regret to say, but the manuscript does not seem to be ready to be published. Thorough revision is still needed. It may be the best to revise the manuscript with professional editors for expression in English, but this does not secure to turn the manuscript well organized. It is still the authors' responsibility that the order of explanations (sentence by sentence) and discussion (paragraph by paragraph and subsection by subsection) need to be well organized prior to the English check in order to make the flow of context smooth in the final form.

Thank you for the opportunity to revise the manuscript to improve clarity, organization and readability.

It is a minor thing, but the column containing “t/h” in Table 2 has also the information of “V/m³”. Those are different information and should be shown in different column.

Since the sample flow was constant, these two values actually represent the same information. However, we follow your recommendation and separated them into two

columns.

I also recommend the authors to show units in brackets instead of slash in this table for consistency (i.e., the slash of “micro g / m³” is meant a division, while the slash of “V/m³” is meant for unit).

In both cases, the slash is division. This is the method recommended by SI, NIST, IUPAC and others, see for example the IUPAC Green Book.

Besides the writing issues, the followings are my responses (underlined) to the authors' comments (Italic) to my previous comments (bold). Please note that I am responding to only the authors' comments that I have opinions on. For those that I am not responding to, it is either of that I am satisfied with the changes or issues are overlapping with those I am already responding to.

Thank you. We will add our response after your underlined comments. We omitted the quoted texts from the last revision for the sake of readability.

General comments

After reading the manuscript, I had impression that points the authors argued were unclear: pieces of discussions seemed to be fragmented.

The discussion was overhauled and there is now a separate section 'Discussion' to allow a clearer distinction between results and discussion. Furthermore, a reaction scheme (new Figure 1) was added as suggested and used to guide the reader through the paper.

Thanks for attempting to revise along my advice, but this change is not satisfactory. I wanted the authors to focus on the important messages that the authors want to tell readers, and logically justify the arguments stepwise using own experimental results and references. The current form seems that the discussion section in the previous manuscript was just divided. The contents and arguments were still confusing. In addition, the “Results” section in the current manuscript substantially includes authors' interpretation and discussion. It is okay to separate the “Results” and “Discussion” sections, but please give only the observed results in the “Results”, and analyze and evaluate own data with references in “Discussion”.

We rearranged some of the content, but there is still some discussion left in the 'Results' section, as this is very hard to be avoided in a paper like this. We have tried many different structures prior to submitting among the authors and in fact didn't want to have them divided until we go the reviewer's comments. Concerning the numbers in Table 5, they are still part of the 'Results' section as they are derived from basic algebra.

I also had impression that some information and discussion (e.g., already studied C:O ratios and natural processes with isotope fractionations) were very detailed, and some (e.g., chemical reactions that lead to formation of low volatility products, calculation for predicted d13C in Table 5) were insufficient.

We have shortened the former and expanded the latter. The calculations leading to the numbers shown in Table 5 are now illustrated with an example and Table 5 was overhauled. The new reaction scheme highlights the reaction pathways that lead to the calculations in Table 5.

I was a bit confused to find “example” illustration for the calculation of position specific d13C of Dgas and Daerosol in Table 5, but the authors

probably meant S5 in the Supplementary Information. I understood that the calculations were based on NMR data, which are for unreacted alpha-pinene. From the revised manuscript, however, I could not retrieve important information to explain the d13C of product Dgas and Daerosol in Table 5 using the position specific d13C of unreacted alpha-pinene.

We have changed the text to make it clear that the values calculated in table five are based on the MCM mechanism presented in Figure 1. Note that the precision of our argument is limited as the branching ratios are not known with certainty as is now pointed out even more clearly, and in any case, will change depending on temperature, pressure, humidity, OH, NO_x and so on. We do not refer to S5 (or NMR data) but Table 5 and it is hard for us to explain the very basic algebra behind the numbers in Table 5 in more simple terms than we have done already. We have however, pointed out the assumptions very clearly at the beginning of the paragraph. The numbers in T5 are derived from the position-specific enrichment listed in Table 2 as described in the text.

The beginning of the passage now reads:

‘Here a limiting case is presented for the isotopic difference of a number of plausible oxidation products. The underlying assumptions exclude isotope dependent changes in product branching ratios, as well as effects of temperature, relative humidity, pressure, ozone concentration, etc. This simplistic approach allows to estimate the maximum isotopic enrichment in a-pinene fragments using the $\Delta i(13C)$ profiles obtained from PSIA.’

In addition, the authors may want to make more focus on what they can conclude from the data they gained. For example, the position-specific isotope analysis (PSIA) sounded a key achievement in the abstract. However, if my understanding is correct, the PSIA was performed only on the unreacted a-pinene. I did not get what conclusion the authors were going to draw from the comparison of this information with d13C of stepwisely evaporated OCs, each of which is still possibly a complex mixture of multiple substances as indicated by more than 400 of fragment ions in the table in S4 of SI. If the authors could identify a specific product possessing enriched/depleted 13C atom at a specific position, which may have originated from a specific position of a-pinene, they should make discussion with the observed evidence (e.g., the difference in d13C between the different samples).

Thank you for your comment. It is correct that PSIA was performed on the unreacted a-pinene only. PSIA on single components of the SOA mixture is not possible at this moment. The argument is that if one dominant reaction channel prefers a certain reaction site on the alpha-pinene, then the position specific isotope distribution might govern the overall isotope signature. However, we cannot fully conclude that. PSIA on a-pinene was performed for the first time and we believe that this is an important result for future research and therefore chose to leave it in the abstract. Other parts of the abstract and large parts of the introduction were rewritten. A reaction scheme was added to better guide the reader in the introduction specifically when it comes to the idea that PSIA could play a role in the ‘bulk’ isotopic composition. Biased 13C distribution in intra molecular carbons of pinene is interesting, and I am not going to be offensive against this finding. However, again, my point is that it is not clear how this PSIA is related to the product analysis presented in this paper. It is reasonable that the authors will combine this result with results of future compound-

specific product study to explore isotope balance between the products, but those are not available at this moment. The presentation of the result here may be justified if D_{gas} and D_{aerosol} in Table 5 were calculated based on the measurement results of PSIA with reasonable assumptions. However, the assumptions (i.e., “maximum expected enrichment” and “branching ratios do not influence the isotopic composition of products”) do not sound. According to Hoefs (1997), the initial isotope ratio, the degree of processing, and the fractionation factor are needed to calculate the isotope ratio of a processing substance or product at any arbitrary time. Presumably, the authors assumed ~ 100% of degree of alpha-pinene oxidation (“completion” in the text probably suggests this), however, this does not secure that the complex subsequent reactions also completed, depending on relative reaction speeds (relative to the speed of ozonolysis of alpha-pinene) of subsequent reactions leading to the production of formaldehyde, acetone, CO, and other products. That is, branching reactions significantly influence product isotopic composition, unless otherwise there is no isotope fractionation (i.e., KIE = 0 permil) at all of these reactions. If even only one of these branching reactions had a significant KIE, which seems more reasonable assumption according to Fisseha et al. (2009), this KIE will significantly influence the isotopic composition of remaining alpha-pinene or intermediate(s) as reactions proceeded. This varying isotopic composition of precursors will then influence the isotopic composition of products from other branching reaction channels because all or a part of products originate from the same precursor.

In the text, it is not clear what substances are defined as “aerosol” and “gasphase”, what number of KIEs and branching ratios were used for the calculation. I am not sure what “the maximum expected enrichment” is, but if the authors assume zero of KIEs at all branching reactions and no branching reactions, I disagree with the assumptions. From the text I could not retrieve those information.

It would be great data to analyse if one had the opportunity to perform PSIA on several of the product species, however, that was not possible in this experimental setup and has to be left for further studies. In the meantime we only have the starting picture (PSIA of alpha-pinene) and the end point (bulk δ values of SOA). While maybe not 100 % satisfying, the best we can do with these fragments is to figure out the potential effect, or so to say how much of the starting picture is left at the end. The presented results demonstrate conclusively that both PSIA and isotope dependent product branching ratios must be considered in studies of isotopic fractionation in SOA formation reactions, especially for natural products.

The assumptions made behind the numbers in Table 5 are of course not perfect, but our goal here was to get an estimate of the potential size of the effect. The branching ratios in the alpha pinene ozonolysis mechanism are unknown and very importantly, the branching ratios will depend on temperature, relative humidity, and the concentrations of ozone, OH, NO_x and other species. We applied a simplification to a complex mechanism, and we did that for the first time with strong results.

Concerning the product branching ratios anything is possible. We argue in the text one reaction having a very large KIE is not likely based on mechanistic considerations (standard addition reactions to a large molecule) and on e.g. the experimental results of e.g. Anderson et al. 2004 and similar papers. The anomalously large KIE's seen in e.g. the ozone formation reaction are anomalies. In line with this, Fisseha et al.'s KIE is for the initial ozonation reaction, not for subsequent reactions, up to our understanding. The assumption to neglect the isotope effects of the branching ratios is not as far-fetched as it may seem at first.

Lack of reaction mechanism for production of SOA from ozonolysis of pinene was also a problem to follow the discussions.

Thank you for your comment. We made a new figure (Fig. 1) that identifies how the site-specific α -pinene $d_{13}C$ values propagate through the reaction mechanism highlighting some key arguments of our paper.

Thanks for providing the reaction scheme. This will definitely make readers easier to follow the discussion. However, the scheme is incomplete and not reader-friendly to follow the reaction steps producing high and low volatility products. For example, taking a look at the production mechanism of pinonic acid and pinoaldehyde in Fig. 1, I don't know what was changed after the second processing step, "stabilization". I see that the red star mark on the carbon disappeared after the step, but what does this mean? I also don't get how "H₂O" was involved in the subsequent reaction after the "stabilization". The same problem for the reaction with RO₂ and HO₂. The authors may want to check how other papers are presenting those reaction schemes. Second point is that the figure also does not show important elemental steps for the production of small products shown in the boxes in Fig. 1. The hidden reaction channels seem to involve reactions with C atoms, thus, must be key steps to explain the results of $d_{13}C$ calculations. Third point is that it is helpful for readers to see branching ratios in the figure.

Considering point 1, the mechanism presented in Figure 1 is consistent with the best available understanding, as found in the Master chemical Mechanism and in the paper we reference (Camredon et al., 2010). By quoting these references, we also invite the reader (and reviewer) to read the literature on the known reactions in case they are not presented in enough detail. The high complexity of the involved reactions disallows much more simplified representations.

Points 2 and 3: Many people would like to know these branching ratios and the elementary steps of the reactions, but they are not known and might never be. Many experiments have only been able to detect products, and even with this information, it is ambiguous what the exact contribution from each branch of the mechanism is. We would happily include this information if it was available to a level of detail that was helpful to interpreting our results, however, this is not the case, up to our knowledge.

Specific comments

P3110: The authors may want to use a symbol of alpha instead of epsilon for the expression of fractionation factor.

We rewrote the section in question and now describe the Kinetic Isotope Effect (KIE) using ϵ values, as is common practice. We believe this makes the explanation easier to follow and more clear. The replacement of ϵ by α does not change the manuscript as they are simply related by $\epsilon = \alpha - 1$ which is common knowledge within the field of isotope research (see for example Coplen, 2011).

Regarding the definition of kinetic isotope effects, Coplen (2011) defines a kinetic isotope effect as $^{12}k/^{13}k$, while Hoefs (1997) defines a fractionation factor as $^{13}k/^{12}k$. The authors may want to stick to either of these.

The paragraph was completely rewritten, see above.

Section 3.1.: The authors may want to present an example time series plot of ozone mixing ratios and pinene concentrations.

Among authors we discussed providing a plot of the ozone mixing ratios but

decided against it. The main reason against it being an interference of organic vapours on the ozone detection system yielding spikes of the ozone mixing ratios. This was tested and confirmed in extra experiments, but with no conclusion / suggestion on how to resolve the issue or how to correct our data for it.

In order to avoid an extended discussion on operation and detection mechanisms of ozone monitors, we opted to leave the plot out. The pinene concentration was not measured.

It is very important to have information of pinene concentration change over time at least. Is it possible to present such info based on MCM calculation with given experimental condition?

Based on the ozone concentration, the reaction rate of α -pinene with ozone and the length of the experiment, we are confident that all of the α -pinene has reacted, as we state in Section 2.3.

In addition, according to Fig 7a, OC at 100 degree Celsius (7% of TC) has the largest difference of -3 permil in $\delta^{13}C$. Any discussion for this difference? Does this difference attribute to different isotopic composition of different chemical species? This is the part the authors should make deeper discussion, I think.

We suspect the reviewer was commenting on panel b of that Figure and will give our answer accordingly. The second last paragraph of section 3 discusses the strong enrichment observed at 100 C. However, the discussion has to stay vague as no clear conclusions can be drawn from the data. Unfortunately, no species or group of species could be assigned to this enrichment. We omitted the last part of the paragraph which dealt with the back filters and added another consideration based on oligomerisation.

Sorry for confusion. It is correct that I was pointing on the panel b. I think it is not necessary to deeply argue with speculation, if there is no reasonable scientific explanation for the difference. However, it is important to point out the difference explicitly and briefly state possible reasons for the difference so that others can hint for future studies to progress the science.

The section was removed.

P16120-33: There are papers discussing site specific isotope fractionations. Why do the authors argue with reactive isotope fractionations using the reference of sorption isotope fractionation of vanillin?

There is not much literature available on the topic as the analysis technique is rather new. However, we now included the Botosoa et al., 2009b reference in the text and omitted speculations about bond length variations.

I am not sure if we are misunderstanding our comments each other, but I can find references for position specific carbon isotope fractionation at different types of chemical reactions (not for physical phenomena), such as Singleton and Szymanski (1999, JACS) and etc. Because the authors are discussing “carbon isotope fractionation” there, it is not necessary to compare only with the results obtained by NMR measurements. Carbon KIEs for elemental reactions obtained by different techniques have been studied for long, some of those may be comparable. Of course, the current reference is also okay, I think.

Thank you, we agree that the reference we chose is appropriate.

Chemical and isotopic composition of secondary organic aerosol generated by α -pinene ozonolysis

Carl Meusinger¹, Ulrike Dusek^{2,3}, Stephanie M. King^{1,4}, Rupert Holzinger², Thomas Rosenørn^{1,5}, Peter Sperlich^{6,7}, Maxime Julien⁸, Gerald S. Remaud⁸, Merete Bilde^{1,9}, Thomas Röckmann², and Matthew S. Johnson¹

¹Department of Chemistry, University of Copenhagen, DK 2100, Copenhagen Ø, Denmark

²Institute for Marine and Atmospheric research Utrecht (IMAU), Utrecht University, 3584 CC, Utrecht, The Netherlands

³Centre for Isotope Research, Energy and Sustainability Research Institute Groningen, 9747 AG Groningen, The Netherlands

⁴now at: Haldor Topsøe A/S, DK 2800, Kgs. Lyngby, Denmark

⁵Infuser ApS, DK 2200, Copenhagen N, Denmark

⁶Max-Planck Institute for Biogeochemistry, 07745 Jena, Germany

⁷now at: National Institute of Water and Atmospheric Research (NIWA), Wellington 6021, New Zealand

⁸CEISAM, UMR CNRS6230, BP 92208, Nantes 44322 cedex 3, France

⁹now at: Aarhus University, Department of Chemistry, 8000 Aarhus C, Denmark

Correspondence to: C.M. (c.meusinger@gmail.com)

Abstract.

Secondary organic aerosol (SOA) plays a central role in air pollution and climate. However, ^[.1]the description of the sources and mechanisms leading to SOA is elusive despite decades of research. ^[.2]While stable isotope analysis is increasingly used to constrain sources of ^[.3]ambient aerosol, in many cases it is difficult to ^[.4]apply because neither the isotopic composition of ^[.5]aerosol precursors nor the fractionation of aerosol forming processes is well characterised. In this paper, SOA formation from ozonolysis of α -pinene - an important precursor and perhaps the best-known model system used in laboratory studies - was investigated using ^[.6]position dependent and average determinations of ¹³C in α -pinene, and advanced analysis of reaction products using thermal-desorption proton-transfer-reaction ^[.7]mass-spectrometry (PTR-MS).

The total carbon (TC) isotopic composition $\delta^{13}\text{C}$ of the initial α -pinene was measured, and the $\delta^{13}\text{C}$ of the specific carbon atom sites was determined using position-specific isotope analysis (PSIA). The PSIA analysis showed variations at individual positions from -6.9 to +10.5‰ relative to the bulk composition. SOA was formed from α -pinene and ozone in a constant-flow chamber under dark, dry and low-NO_x conditions, with OH scavengers and in the absence of seed particles. The excess of ozone and long residence time in the flow chamber ^[.8]ensured that virtually all ^[.9] α -pinene ^[.10]had

¹removed: an exact

²removed: Stable

³removed: the ambient aerosol. However

⁴removed: draw firm conclusions

⁵removed: many aerosol sources

⁶removed: stable carbon isotope analysis, and high-resolution chemical analysis based on a

⁷removed: mass-spectrometer

⁸removed: was long enough

⁹removed: initial

¹⁰removed: has

reacted. Product SOA was collected on [..¹¹]two sequential quartz filters. The filters were analyzed offline by heating them
5 stepwise from 100 to 400 °C to desorb organic compounds that were (i) detected using PTR-MS for chemical analysis and to
determine the O:C ratio, and (ii) converted to CO₂ for ¹³C analysis. [..¹²]

More than 400 ions in the mass range [..¹³]39-800 Da were detected [..¹⁴]from the desorbed material and quantified using
a PTR-MS. The largest [..¹⁵]amount desorbed at 150 °C. The [..¹⁶]O:C ratio of [..¹⁷]material from the front filter increased
from 0.18 to 0.25 as the desorption temperature was raised from 100 to 250 °C. [..¹⁸]At temperatures above 250 °C the O:C
10 ratio of thermally desorbed material, presumably from oligomeric precursors, was constant. The observation of a number
of components that occurred across the full range of desorption temperatures suggests that they are generated by thermal
decomposition of oligomers.

[..¹⁹]The isotopic composition of SOA was more or less independent of desorption temperature above 100 °C. TC analysis
showed that SOA was enriched in ¹³C by 0.6-1.2‰ relative to the initial α-pinene. [..²⁰]According to mass balance gas
15 phase products will be depleted relative to the initial α-pinene. [..²¹]Accordingly, organic material on the back filters, which
contain adsorbed gas phase compounds [..²²], is depleted in ¹³C in TC by 0.7‰ [..²³]relative to the initial α-pinene, and by
1.3‰ compared to SOA collected on the front filter. The observed [..²⁴]difference in ¹³C between the gas and particle [..²⁵
]phases may arise from isotope-dependent changes in the [..²⁶]branching ratios in the α-pinene + O₃ reaction. Alternatively,
some gas phase products involve carbon atoms from highly enriched and depleted sites as shown [..²⁷]in the PSIA analysis, [..²⁸
20]giving a non-kinetic origin to the observed fractionations. In either case, the present study suggests that the site-specific
distribution of ¹³C [..²⁹]in the source material itself governs the abundance of ¹³C in SOA.

¹¹removed: doubly-stacked quartz filters(the front and back filters). During subsequent offline analysis, the filters were heated

¹²removed: In addition, the total carbon (TC) isotopic composition of selected samples was measured and position-specific isotope analysis (PSIA) was
performed on the initial α-pinene. The PSIA analysis showed variations in isotope enrichment at individual carbon positions in α-pinene from -6.9 to +10.5‰
relative to the bulk composition.

¹³removed: from

¹⁴removed: and quantified in

¹⁵removed: mass fraction desorbed from the filters

¹⁶removed: measured

¹⁷removed: front filter material

¹⁸removed: The rising trend is consistent with the fact that functionalization decreases the volatility of chemical species.

¹⁹removed: At desorption temperatures above 100 °C the

²⁰removed: Since all α-pinene has reacted this implies that the gas phase compounds should be depleted with respect

²¹removed: Consistently, the analysis of

²²removed: indicates that these compounds are

²³removed: compared

²⁴removed: isotopic difference between

²⁵removed: phase in ¹³C could be explained by kinetically-derived

²⁶removed: product branching ratios, or by considering that

²⁷removed: by

²⁸removed: or by a combination of these (and other factors including the effect of isotopic substitution on volatility and oligomerisation). Overall, this
study provides an important link by using

²⁹removed: to connect a carefully characterised precursor to SOA by a defined mechanism.

1 Introduction

Secondary Organic Aerosol (SOA) is formed in the atmosphere by oxidation of Volatile Organic Compounds (VOC's). SOA contributes significantly to ³⁰atmospheric aerosol and impacts climate, air quality and health (Stocker et al., 2013; Hänninen et al., 2004; Dockery et al., 1993; Andreae and Crutzen, 1997). ³¹Despite their impacts the mechanisms of SOA formation and processing are poorly understood and significant discrepancies between model predictions and observations are common.

Stable carbon isotopes are increasingly used to investigate ³²aerosols in the atmosphere. Isotopic analysis holds the promise of clearly identifying SOA sources and atmospheric transformations, if only we knew enough details, such as the isotopic composition of the source emissions, the kinetic fractionations occurring in oxidation reactions, and the isotope effects in phase partitioning. The ability to distinguish individual sources, including marine aerosol (Turekian et al., 2003; Ceburnis et al., 2011) and biomass burning (Kirillova et al., 2013), by isotope measurements has been particularly useful when it comes to source apportionment of ambient aerosol (e.g., Sakugawa and Kaplan, 1995; Narukawa et al., 2008; Turekian et al., 2003; Widory et al., 2004; Ho et al., 2006; Huang et al., 2006; Fisseha et al., 2009; Kirillova et al., 2013; Ceburnis et al., 2011; Fu et al., 2012; Miyazaki et al., 2012; O'Dowd et al., 2014; Masalaite et al., 2015).

³³In some other cases, measurements of the isotopic composition of SOA ³⁴have yielded intriguing and/or contradictory results: Irei et al. (2014) found that SOA formation from oxidation of volatile organics lead to depletion in ¹³C in the low-volatile fraction of the aerosol. Fu et al. (2012) on the other hand reported isotopic ³⁵enrichments in ambient SOA that ³⁶are distinguishable between biomass burning and primary emissions, possibly hinting at the oxidation of biogenic VOC.

³⁷³⁸

³⁰removed: the aerosol burden of the atmosphere and has impacts on climate, health and visibility

³¹removed: The formation and processing of SOA in the atmosphere encompasses a complex array of chemical and physical processes, like condensation, evaporation, water uptake, and reactions on the particle surface, rendering it difficult to determine the sources of SOA and predict the effect of SOA on climate and health.

³²removed: the processing and sources of aerosols in the atmosphere. The possibility

³³removed: An incomplete understanding of how atmospheric processes influence isotopic abundances has however limited the use of isotope information in constraining SOA contributions to the aerosol burden. While the interpretation of ambient measurements could benefit from the better characterisation of sources, especially the inferred

³⁴removed: has yielded

³⁵removed: enrichment

³⁶removed: is distinguishable from

³⁷removed: Different chemical and physical processes fractionate isotopes, and could lead to isotopic enrichment (or depletion) in SOA with respect to the precursor. Carbon isotopic fractionation changes the ¹³C/¹²C ratio of a sample (Coplen, 2011). Briefly, there are two types of isotopic fractionation: equilibrium and kinetic fractionation. Equilibrium fractionation describes the change in the isotopic composition due to unequal partitioning of isotopic analogues of a compound (isotopologues) between two phases. Equilibrium fractionation is important for light molecules because the extra neutron in isotopes like ²H, ¹⁷O, ¹³C significantly adds to the molecular mass of the compound. Monoterpenes and their oxidation products have large molecular masses relative to the added 1

³⁸removed: in ¹³C and the isotopic equilibrium fractionation due to their gas/particle partitioning becomes negligible (Gensch et al., 2011; Irei et al., 2011).

[..³⁹]

Recent technical advances have made it possible to quantify isotopic enrichments at specific sites within molecules, in addition to the traditional determination of the enrichment of the sample itself (Bayle et al., 2014b). This development makes possible new analyses of chemical mechanisms and transformations in the environment. Consider a chemical reaction that goes to completion to give a variety of products. The atoms of a reagent are distributed among the products, depending on the branching ratios for the different reaction channels. The branching ratios may themselves be isotope dependent. For the formation of SOA from a VOC precursor, the isotopic enrichments/depletions that are observed in the

5 [..⁴⁰] SOA arise from the contributions of many oxidation products. Mass balance implies that the complimentary pattern will be observed in gas phase products. Many interesting research questions arise from the application of site-specific isotopic analysis to atmospheric science, perhaps most importantly, is the observed average composition of the SOA due to the isotope dependent changes in product branching ratios within the reaction mechanism, or, is it due to the site-specific enrichments of the reagent?

10 Isotopic substitution can cause reactions to be faster or slower than for the unsubstituted case, kinetically fractionating the isotopes and leading to isotopic enrichment or depletion in the products. This is known as the kinetic isotope effect (KIE). If a reaction leads to a single product, the product may initially have a different abundance, but due to the law of mass balance will achieve the same abundance as the reagent as the reaction goes to completion. If a reaction has multiple product channels, enrichment or depletion will occur if there are isotope dependent changes in the product

15 branching ratios.

The ozonolysis of α -pinene is often used as a test system for formation of SOA; it is fairly well studied. Figure 1 shows a reaction scheme for α -pinene ozonolysis, based on the Master Chemical Mechanism (MCMv3.1) as described by Camredon et al. (2010). In the first step ozone adds into the double bond of the molecule resulting in two branches depending on the usual Criegee mechanism. These two branches proceed by stabilisation, and subsequent fragmentation and isomerization, and sub-

20 sequent reaction with RO_2 , HO_2 and H_2O to yield a wide range of oxidation products from CO, HCHO and acetone, to many larger oxidised low volatile molecules like pinic acid and pinonic acid and pinonaldehyde. The figure shows only formation of first generation products. Further reactions including dimer formation (Kristensen et al., 2016) and oligomerization reactions are not shown.

Generally, reactions involved in atmospheric VOC oxidation fall into three categories: functionalization, fragmentation and oligomerization (Kroll and Seinfeld, 2008; Rudich et al., 2007; Chacon-Madrid and Donahue, 2011). The volatility (Donahue

³⁹removed: Kinetic fractionation results from isotope-dependent differences in reaction rates. Let ^{12}k denote a reaction rate constant for a reaction involving a compound containing only ^{12}C and let ^{13}k denote the reaction rate constant for the reaction involving a single-substituted ^{13}C isotopologue; the kinetic isotope effect (KIE) can be written as $\epsilon = ^{13}k/^{12}k - 1$. It is common to distinguish "normal" and "inverse" KIEs. During normal kinetic fractionation the extra neutron slows chemical reactions (Johnson et al., 2002) and ϵ becomes negative (this definition follows the definition of the δ -value in Sect. 2.5.2 but different definitions exist in the literature). Over the course of the reaction the reactant is successively enriched in heavy ^{13}C and the oxidation product is depleted. Conversely, during inverse kinetic fractionation $\epsilon > 1$, depleting the reactant and enriching the product. Once the reaction has come to completion with no reactants left, and assuming no branching to other product channels,

⁴⁰removed: isotopic composition of the product will be identical to that of the reactant at start (for both normal and inverse kinetic fractionation) to satisfy mass balance

et al., 2006; Jimenez et al., 2009) and oxygen-to-carbon ratio, O:C (Donahue et al., 2011; Kroll et al., 2011), of involved species allow characterising these processes. The characteristics of the three types of atmospheric VOC reactions and ^[..⁴¹]current understanding of how they contribute to isotopic fractionation (Kirillova et al., 2013, 2014) are summarised as follows:

- 5 – Functionalization describes the addition of oxygenated functional groups to the parent compound. A typical example is the first reaction step in VOC oxidation. In these reactions, products are less volatile and have higher O:C ratios than the parent compound. Functionalization is typically accompanied by normal kinetic fractionation leading to oxidation products depleted in ¹³C (Rudolph and Czuba, 2000; Iannone et al., 2010; Gensch et al., 2011). In the present study, the parent compound α -pinene was fully oxidised leaving no isotopic imprint on its products (the KIE of α -pinene
- 10 ozonolysis has not been reported to date).
- Fragmentation describes cleavage of carbon-carbon bonds possibly followed by addition of oxygen to the fragments. Fragmentation reactions in the condensed phase can result in molecules that are small, like CO₂ and CH₂O, have higher volatilities than the parent compound and might escape to the gas phase (Kroll et al., 2009). ^[..⁴²]Fragmentation may enrich the aerosol in ¹³C ^{through normal kinetic fractionation}: when some of the depleted reaction products are lost
- 15 to the gas phase the remaining aerosol phase will be enriched (Aggarwal and Kawamura, 2008). The O:C ratio of the products is often higher than for the parent VOC and is typically highest for compounds remaining in the aerosol phase. During ozonolysis of monoterpenes both functionalization and fragmentation occur simultaneously (Chacon-Madrid and Donahue, 2011), as also shown in Fig. 1. This increases the O:C ratio but the overall effect on the isotopic balance is not well established.
- 20 – Oligomerization (sometimes also referred to as accretion) describes the building of larger organic structures from monomers, often in the aerosol phase (Kalberer et al., 2004, 2006; Hallquist et al., 2009). ^[..⁴³]One mechanism is that oxygenated organics become linked by dehydration reactions, and this lowers the O:C ratio^[..⁴⁴]. The formation of complex organic mixtures in the aerosol phase (Cappa et al., 2008) is expected to show similar characteristics in vapour pressure and O:C ratio. The influence of oligomerization on the isotopic composition of the aerosol is not
- 25 clear^[..⁴⁵], but likely small.

Chemical analysis based on proton-transfer-reaction mass spectrometry has proven very useful in ambient and laboratory studies investigating aerosol and gas-phase compounds and their properties (e.g., Holzinger et al., 2010a, b; Shilling et al., 2008; Presto and Donahue, 2006). Advantages of the technique include the soft ionisation, high sensitivity, wide range of detectable compounds, and the possibility of quantifying them. ^[..⁴⁶]In addition, using a proton-transfer-reaction time-of-flight mass

⁴¹removed: the current understanding on

⁴²removed: During fragmentation normal kinetic fractionation can

⁴³removed: The

⁴⁴removed: remains constant during oligomerization while the vapour pressure of the products drops significantly

⁴⁵removed: .

⁴⁶removed: Using

spectrometer (PTR-ToF-MS, shortened to PTR-MS for the remainder of the article) [..⁴⁷] allows chemical characterisation and identification of compounds and estimation of the O:C ratio.

Position-specific isotope analysis (PSIA) of the initial reactant offers [..⁴⁸] a detailed description of bulk isotopic data [..⁴⁹] by mapping the intra-molecular isotope distribution. PSIA by ¹³C isotope ratio monitoring by NMR (irm-¹³C NMR) has proven valuable in interpreting a number of (bio)chemical (Bayle et al., 2014a; Botosoa et al., 2009a; Gilbert et al., 2011, 2012) and physical-chemical processes such as distillation and sorption (Botosoa et al., 2008, 2009b; Höhener et al., 2012), leading to a deeper understanding of the underlying phenomena causing isotope fractionation in nature. [..⁵⁰] It is widely understood that the enrichment/depletion of a product depends on the enrichment of the starting material, the isotopic fractionation occurring in the mechanism of its formation, and the extent of reaction. Using PSIA we can take this analysis one step further: the enrichment of a product will depend on the position-dependent enrichments of the atoms from which it is formed. For example the ozonolysis mechanism transfers the C₉-atom in α -pinene into several small, volatile [..⁵¹] products (see blue squares in Fig. [..⁵²] 1). If [..⁵³] the C₉-position was depleted in ¹³C [..⁵⁴] the gas phase [..⁵⁵] products containing this atom would be depleted, and the SOA correspondingly enriched, if the position dependent effect was stronger than kinetic isotope effects.

The goal of this study [..⁵⁶] is to provide detailed isotopic and chemical characterization of newly formed α -pinene SOA and to shed light on the mechanisms that govern isotopic fractionation in the formation of fresh SOA.

2 Material and methods

2.1 Chemical compounds used

Chamber experiments were performed using the following chemicals: (+)- α -pinene (Aldrich, > 99%, batch #80796DJV), 1-Butanol (Sigma-Aldrich, > 99.4%) and cyclohexane (Labskan, 99.5%). PSIA was performed on several samples of α -pinene from Sigma-Aldrich, Acros Organics, Merck, and Alfa Aesar, see Table 1. The batch of α -pinene used in the chamber experiments could not be analysed using PSIA, because the manufacturer does not supply it anymore.

⁴⁷removed: additionally

⁴⁸removed: another way of understanding

⁴⁹removed: . A microscopic view of the isotopic composition is made possible

⁵⁰removed: The position-specific isotope composition could yield unexpected isotopic fractionation in atmospheric aerosol. For example, the C₉-atom in α -pinene is found in many

⁵¹removed: ozonolysis products as it is expelled preferentially solely due to its position during fragmentation reactions

⁵²removed: 1

⁵³removed: for example the C₉-position

⁵⁴removed: this could lead to depletion of

⁵⁵removed: not caused by kinetic fractionation

⁵⁶removed: was

2.2 Chamber design and characteristics

A new aerosol smog chamber was built in Copenhagen based on a steady-state design (King et al., 2009; Shilling et al., 2008; Kleindienst et al., 1999). It consists of a 4.5 m³ teflon bag (the volume/surface ratio is 0.275 m) mounted inside a temperature controlled insulated room of walk-in size (Viessmann A/S) see Fig. S1 in the supplementary information (SI). While details can be found in SI Sect. S1, chamber operation is briefly summarised here. The chamber was operated in a constant-flow mode^[..⁵⁷]; dry air and reactants were flushed into the chamber constantly using mass flow controllers. A syringe pump (NE-300, New Era Pump Systems Inc.) continuously injected a mixture of α -pinene and 1-butanol or a mixture of α -pinene and cyclohexane into a warmed glass bulb. 1-butanol and cyclohexane were used as OH scavengers and the mixing ratio between α -pinene and the OH scavenger was 1:600 (v/v). A small flow of clean, dry air (0.1 L/min) directed over a Hg lamp emitting UV light (model 600, Jelight company Inc.) generated ozone which was fed into the chamber separately.

Generated aerosol was sampled after an ozone scrubber on doubly stacked quartz-fibre filters (4.7 cm diameter, QMA 1851, Whatman) for offline chemical and isotope analysis at 10 L/min. Collection times were around 1-2 days in order to provide sufficient amounts of carbon on the filters for isotope analysis, see Table 2. The ozone scrubber had a denuder design and used potassium iodine (Williams and Grosjean, 1990). It protected instruments from high ozone levels but also precluded further reaction of collected samples with ozone on the filters.

Several instruments^[..⁵⁸] monitored gaseous and particulate matter inside the bag: a scanning mobility particle sizer, SMPS (TSI 3081 DMA and 3772 CPC, 0.0508 cm impactor) was used to measure particle size distributions (10-500 nm diameter if not stated otherwise) and a cloud condensation nuclei counter (CCNC, Droplet Measurement Technologies) gave information on the CCN properties of generated SOA (King et al., 2012). Temperature and relative humidity were measured continuously inside the bag (Hygroflex HF532, Rotronic) and read by the same software that controlled the pressure inside the bag. NO_x (= NO + NO₂) levels were monitored using a chemiluminescence NO_x analyzer (42i, Thermo). The same line fed^[..⁵⁹] a UV photometric O₃ analyzer (49i, Thermo) to monitor ozone levels.

2.3 α -pinene ozonolysis

All aerosol was generated from the dark ozonolysis of α -pinene under low NO_x conditions (< 2 ppb) without any seed particles present. Experiments were performed with two different OH scavengers: Experiment B with 1-butanol and Experiment C with cyclohexane. The amount of α -pinene injected using the syringe pump resulted in a steady state concentration of ca. 60 ppb inside the bag (without oxidants). Ozone concentrations during the experiment were always above 150 ppb, i.e. ozone was always in excess. The temperature was stable at 22 °C and RH < 1%. Without seed particles present, aerosol formed via new particle formation. Table 2 gives an overview of the conditions under which experiments B and C were performed.

⁵⁷removed: where

⁵⁸removed: were used for characterization of the aerosol and gas phase composition

⁵⁹removed: an

[..⁶⁰] The natural (e-folding[..⁶¹]) lifetime of α -pinene with respect to [..⁶²] ozonolysis is $\tau_{O_3} = (k[O_3])^{-1} = 40$ min based on an ozone concentration of 150 ppb and a second-order rate coefficient of $k = 1.1 \times 10^{-16} \text{ cm}^3 \text{ molecule}^{-1} \text{ s}^{-1}$ (Witter et al., 2002). The nominal residence time of an air parcel in the chamber is $\tau_{\text{nominal}} \approx 3.4$ h (see Sect. S1[..⁶³]) which exceeds the natural lifetime with respect to ozone loss by a factor of five. This means that more than 99 % of α -pinene will have reacted [..⁶⁴] at steady state and for further evaluation and discussion it is assumed that α -pinene ozonolysis was complete. As total mass is conserved for all isotopes, the isotopic composition of the [..⁶⁵] ozonolysis products should be equal to [..⁶⁶] that of the initial [..⁶⁷] reagent.

2.4 Filter handling protocol

Glass vials with plastic stoppers were used to store the quartz filters for off-line analysis before and after the experiments. The glass vials themselves were cleaned in a ceramic oven at 600 °C for 24 h prior to use. The quartz filters were cleaned in the same oven at 600 °C for more than 20 h prior to use. Each filter was stored in a separate glass vial that was wrapped in aluminium foil and stored in a dark freezer (-30 °C) except when loading or during transport between Copenhagen and Utrecht. Two quartz filters (QBQ) were loaded at a time in a cleaned filter holder to account for possible sampling artefacts, such as adsorption and evaporation of organic vapours on / from the filters (Watson et al., 2009; Turpin et al., 2000). In this study the first filter, facing the sample stream, is called the *front* filter, while the second one (stacked below) is called the *back* filter. Storage time between loading and analysis was up to six months. During transport the filters stayed in the wrapped vials but were not actively cooled. Prior to analysis the filters were cut into pieces of uniform size (0.5 and 1 cm diameter). Blank filters were treated identically to loaded filters but were not exposed to chamber air. Gloves were used whenever working directly with the filters and all tools were rinsed several times using first acetone, and then ethanol.

2.5 Filter analysis

The [..⁶⁸] filter samples from the smog chamber experiments were analyzed for their chemical and isotopic composition at the Institute for Marine and Atmospheric research Utrecht (IMAU). Propagated uncertainties based on at least three measurements are given as 1-sigma errors. Filters ID's are composed of a capital letter denoting the experiment (B using 1-butanol or C using cyclohexane as OH scavenger), a digit counting the experiments using that scavenger and a small letter indicating the filter position: *b* for back filter and *f* for front filter.

⁶⁰removed: The

⁶¹removed: time

⁶²removed: loss to ozone

⁶³removed: in the SI

⁶⁴removed: during this time

⁶⁵removed: initial ozonolysis product

⁶⁶removed: the one

⁶⁷removed: reactant. As a consequence, the isotopic composition of generated SOA will not be influenced by the (unknown) kinetic isotope effect of the initial functionalization reaction in ozonolysis.

⁶⁸removed: filters with

2.5.1 Thermal-desorption chemical analysis of filters

The chemical analysis [..⁶⁹] follows methods described earlier (Holzinger et al., 2010b; Timkovsky et al., 2015) and will only be outlined briefly here. The chemical analysis setup consisted of a two-stage oven. Filter pieces were heated [..⁷⁰] step-wise in the first oven [..⁷¹] to temperatures of 100, 150, 200, 250, 300 and 350 °C, while the temperature of the second oven [..⁷²] was kept constant at 200 °C. SOA [..⁷³] components desorbed from the filters according to their volatility and a flow of nitrogen (50 ml/min) carried them to the PTR-MS (PTR-TOF8000, Ionicon Analytik GmbH, Austria) situated directly after the second oven. The PTR-MS inlet was heated to its maximum temperature of 180 °C, while the drift tube was operated at 120 °C. This [..⁷⁴] monotonic gradient from the first oven stage to the drift tube inside the PTR-MS reduced cold spots and minimised repeated sample condensation. The PTR-MS detected the desorbed compounds after protonation (addition of ¹H) as ions with a mass to charge ratio (m/z) + 1.

10 The PTR-MS had a mass resolution of $m/\Delta m \approx 4000$ allowing detection of ions with differences in m/z larger than 30 mDa. The algorithm for analyzing the PTR-MS data is based on a method reported earlier (Holzinger et al., 2010a; Holzinger, 2015). For each experiment (B or C), the ions detected on the front and back filters were combined in a unified-peak-list to minimise statistical uncertainty and improve overall mass accuracy (Holzinger et al., 2010a). Ions with $m/z < 39$ Da were excluded (except 33.03 Da, methanol, and 31.01 Da, formaldehyde) as the PTR-MS mainly detects primary ions in this mass region, which do not originate from the filters. Water clusters with masses 37.026 and 55.038 Da can form in the PTR-MS and were not considered to be aerosol compounds. A total of 685 (753) ions were detected by the PTR-MS in experiment B (C). In order to take the contribution from the blank filter (filter ID 'HB' for handling blank) into account, the blank filter loading was calculated from the PTR-MS signal and subtracted from the front and back filters for each ion on the unified-peak-list. All ion concentrations are then reported relative to smog chamber conditions, i.e. as mass of detected ion per unit volume of air in the smog chamber. Table 2 lists the blank-corrected total mass concentration, $M_{\text{total}}^{\text{PTR-MS}}$. Many ions had negligible concentrations. [..⁷⁵] The 427 (451) ions from the unified-peak-list of experiment B (C) comprising 90 % of the total aerosol mass detected by PTR-MS (counting from the ion with highest concentration downwards) were considered for further analysis in order to streamline data analysis and reduce noise.

25 The data analysis algorithm [..⁷⁶] identified the molecular formulas of the detected ions (i.e. the total number of most abundant stable C, H, O and N isotopes) based on their exact masses. [..⁷⁷] If the peak resolution did not allow unambiguous identification, several candidates were suggested [..⁷⁸] (Holzinger et al., 2010a). The suggested formulas for all prominent peaks

⁶⁹removed: followed

⁷⁰removed: up

⁷¹removed: stage

⁷²removed: stage

⁷³removed: compounds

⁷⁴removed: declining temperature

⁷⁵removed: In order to streamline data analysis and to reduce noise only the

⁷⁶removed: was also used to identify

⁷⁷removed: In cases when

⁷⁸removed: by the algorithm

were checked manually on at least two filters and corrected if necessary, including when the suggested formula contained N or ^{13}C . The former can be excluded due to the low NO_x conditions in the experiment and the latter can be easily verified by the corresponding carbon-12 peak at $(m/z - 1) + 1$. Most of the ions were identified unambiguously and typically only ca. 5 % of the total ion mass from front filter desorption were attributed to ions with no clear molecular formula.

The oxygen-to-carbon ratios [..⁷⁹] of the ions were calculated [..⁸⁰] as in Holzinger et al. (2013) for each filter at each
5 desorption temperature:

$$\text{O:C} = \frac{\sum w_i n_{\text{O},i}}{\sum w_i n_{\text{C},i}} \quad (1)$$

Here, the sum counts over all identified ions i , w_i is the measured amount of ion i in mol and $n_{\text{C},i}$ and $n_{\text{O},i}$ are the respective number of carbon and oxygen atoms for ion i as given by its molecular formula. Equation (1) gives the ratio of oxygen to carbon atoms in all identified ions.

10 2.5.2 Thermal-desorption isotope analysis of filters

The [..⁸¹]system used to measure the carbon isotope composition of the filter samples [..⁸²] consisted of a two stage oven, as described in detail by Dusek et al. (2013). The filter pieces were heated stepwise in the first oven stage to temperatures of 100, 150, 200, 250, 300, 340 [..⁸³] and 390 °C, desorbing [..⁸⁴] SOA compounds according to their volatility. In the second oven stage, the gaseous compounds were [..⁸⁵] oxidised to CO_2 at 550 °C using a platinum wool catalyst. The CO_2 was dried
15 and purified using two cold traps and a GC column before it was analyzed in a Delta plus XL isotope ratio mass spectrometer (Thermo, IR-MS) [..⁸⁶] [..⁸⁷]. The catalyst was charged using pure O_2 and then a [..⁸⁸] filter piece was placed in the oven which was subsequently flushed with helium. The heating of the filter and subsequent purification of CO_2 took place in a helium carrier gas flow. [..⁸⁹] Filter samples were bracketed [..⁹⁰] between blank filter samples. IR-MS detects each isotopologue of CO_2 as a distinct peak with an associated peak area. The $\delta(^{13}\text{C})$ value was calculated from these areas (see below). Reported
20 data were corrected by taking the corresponding blank filter [..⁹¹] measurements into account.

Isotope data are commonly reported in delta notation, using Vienna Pee Dee Belemnite (VPDB), as an element-specific international standard for ^{13}C :

$$\delta(^{13}\text{C}) = \frac{R_{\text{sa}}(^{13}\text{C})}{R_{\text{VPDB}}(^{13}\text{C})} - 1 \quad (2)$$

⁷⁹removed: , O:C,

⁸⁰removed: similarly to the work of

⁸¹removed: setup

⁸²removed: was described in detail by Dusek et al. (2013). The isotope analysis setup also

⁸³removed: ,

⁸⁴removed: different

⁸⁵removed: fully combusted

⁸⁶removed: in continuous flow mode along with

⁸⁷removed: laboratory standards. The measurement procedure followed a protocol where first the

⁸⁸removed: new

⁸⁹removed: In the order of analysis filter

⁹⁰removed: by

⁹¹removed: measurement

Here, $R_{\text{sa}}(^{13}\text{C})$ and $R_{\text{VPDB}}(^{13}\text{C})$ denote the isotope ratios ($^{13}\text{C}/^{12}\text{C}$) in the sample and standard respectively.

In this study isotopic compositions of filter material are discussed relative to the isotopic composition of the initial α -pinene, $\delta_{\text{TC}}^{\circ 1}(^{13}\text{C})$, where TC denotes total carbon analysis (see below). Changes in isotopic composition are then reported as an isotopic difference (Coplen, 2011):

$$\Delta(^{13}\text{C}) = \delta(^{13}\text{C}) - \delta_{\text{TC}}^{\circ 1}(^{13}\text{C}) \quad (3)$$

- 5 $\Delta(^{13}\text{C}) > 0$ indicates enrichment and $\Delta(^{13}\text{C}) < 0$ indicates depletion in ^{13}C with respect to the initial α -pinene.

2.6 Total carbon isotope analysis of α -pinene and selected filters

The α -pinene used in the smog chamber experiments and selected filters (cf. Table 2) were transferred into tin capsules (4x6 mm capsules from Lüdi AG, Flawil, Switzerland), weighed and analysed for total carbon isotopic composition, $\delta_{\text{TC}}(^{13}\text{C})$ in the ISOLAB of the Max-Planck-Institute for Biogeochemistry in Jena, Germany. The analytical setup comprised an elemental analyser (EA-1100, Carlo Erba, Milano, Italy) which was coupled to a Delta+ IR-MS (Finnigan MAT, Bremen, Germany) through a ConFlo III interface (Werner et al., 1999). The complete system was described by Brooks et al. (2003). All $\delta_{\text{TC}}(^{13}\text{C})$ isotope ratios were referenced against the VPDB scale using an in-house working standard which itself is referenced against NBS 22, with a prescribed value of -30.03 ‰ (Coplen et al., 2006). Blank tests within each measurement sequence were used for blank correction. The analytical performance was maintained and monitored according to a measurement protocol that was described by Werner and Brand (2001). The estimated uncertainty of the $\delta_{\text{TC}}(^{13}\text{C})$ analysis was 0.11 ‰, based on long term performance records. The total carbon isotopic composition is reported here as $\delta_{\text{TC}}^{\circ 1}(^{13}\text{C})$ for the initial α -pinene used in the smog chamber experiments and as isotopic difference with subscript TC, $\Delta_{\text{TC}}(^{13}\text{C}) = \delta_{\text{TC}}(^{13}\text{C}) - \delta_{\text{TC}}^{\circ 1}(^{13}\text{C})$, for all other samples.

2.7 Position-specific isotope analysis of α -pinene

- 20 The sample preparation for NMR analysis consisted of the successive addition of 100 μL of a relaxing agent, $\text{Cr}(\text{Acac})_3$ (Merck) at 0.1 M in the lock substance, Acetone- d_6 (EURISOTOP), to a 4 mL vial. Then 600 μL of pure α -pinene was added and the mixture was introduced into a 5 mm NMR tube. Quantitative ^{13}C NMR spectra were recorded using a Bruker AVANCE III connected to a 5 mm i.d. BBFO probe tuned to the recording frequency of 100.62 MHz. The temperature of the probe was set to 303 K, without tube rotation. The acquisition conditions were those recommended in previous works (Bayle et al., 2014b; Silvestre et al., 2009) and are detailed in Sect. S5[.92]. Isotope $^{13}\text{C}/^{12}\text{C}$ ratios were calculated from processed spectra (cf. Fig. S4 in SI) as described previously (Bayle et al., 2014b; Silvestre et al., 2009), cf. Sect. S5[.93]. The measured position-specific isotopic compositions are given in delta-notation and denoted as $\delta_i(^{13}\text{C})$ where i denotes the position of the C-atom, cf. Fig. 7. Typical accuracy of $\delta_i(^{13}\text{C})$ is 1 ‰.

⁹²removed: in the SI

⁹³removed: in the SI

Total carbon isotopic abundance, $\delta_{\text{TC}}^{\circ j}({}^{13}\text{C})$, was determined by IR-MS using an Integra2 spectrometer (Sercon Instruments, Crewe, UK) linked to a Sercon elemental analyser. Here, j denotes different α -pinene samples as listed in Table 1 (PSIA was only performed for samples $j = 2..5$). A precision balance (Ohaus Discovery DV215CD) has been used to introduce 0.5 mg of pure α -pinene into tin capsules (2x5 mm, Thermo Fisher scientific), before loading them into the elemental analyser. The instrument was referenced against the VPDB scale using international reference materials NBS-22 ($\delta_{\text{VPDB}}({}^{13}\text{C}) = -30.03\text{‰}$),
5 SUCROSE-C6 ($\delta_{\text{VPDB}}({}^{13}\text{C}) = -10.80\text{‰}$), and IAEA-CH-7 PEF-1 ($\delta_{\text{VPDB}}({}^{13}\text{C}) = -32.15\text{‰}$) (IAEA, Vienna, Austria). Instrumental deviation was followed via a laboratory standard of glutamic acid. The corresponding position-specific isotopic difference is reported as $\Delta_i({}^{13}\text{C}) = \delta_i({}^{13}\text{C}) - \delta^{\circ j}({}^{13}\text{C})$.

3 Results

3.1 Aerosol characteristics

10 The evolution of SMPS-derived size-distributions and total mass concentrations over time show that [..⁹⁴]the aerosol population inside the bag was nearly constant for several days after the first day, cf. Fig. S2 and panel a in Fig. S3[..⁹⁵]. Sampling on filters was started ca. 24 h after [..⁹⁶]the injection of VOCs into the chamber. The [..⁹⁷]CCN activity of SOA generated in this study resembles literature data for α -pinene SOA generated in batch mode chambers (panel b in Fig. S3[..⁹⁸]). The integrated SMPS size distribution provides an estimate of the total SOA mass concentration in the chamber[..⁹⁹], 22 and 25 $\mu\text{g}/\text{m}^3$ for
15 experiment B and C, respectively, although particles larger than 500 nm are not accounted for. A detailed characterisation of the chamber aerosol can be found in Sect. S2[..¹⁰⁰].

3.2 Chemical composition

3.2.1 Blank filter

Very low surface loadings (0.23 $\mu\text{g}/\text{cm}^2$) were found on the blank filter (HB), cf. Table 2. No peaks above 220 Da were detected.
20 $\text{C}_3\text{H}_6\text{OH}^+$ (corresponding to protonated acetone) was the only compound found on the blank filter in concentrations above 5 ng/cm^2 at 100 °C while all other ions showed temperature-independent concentrations below that. High concentrations of acetone desorbed from all filters at 100 °C and [..¹⁰¹]may be an artefact from cleaning[..¹⁰²], although acetone is produced in the reaction as shown in Figure 1. The total surface loadings of the front and back filters always exceeded those on the

⁹⁴removed: ca. one day after start of the experiment the

⁹⁵removed: in the SI

⁹⁶removed: start of

⁹⁷removed: measured

⁹⁸removed: in the SI

⁹⁹removed: of

¹⁰⁰removed: in the SI

¹⁰¹removed: are likely

¹⁰²removed: . When handling the filters, some of the acetone used to clean the tweezers stayed on the filter and evaporated at the first temperature step.

blank filter except for single ions with [..¹⁰³] concentrations near the detection limit, sometimes found desorbing from back
25 filters at temperatures other than 150 °C. Correction for the blank filter concentration then resulted in negative concentrations
for these ions for the back filters. These cases were neglected in the further data analysis.

3.2.2 Concentration thermograms

Figure 2 shows the sum of ion concentrations at each temperature step as measured by PTR-MS. All front filters (B1f, B2f,
C1f, and C2f) show a similar profile with most of the mass desorbing at 150 °C. The back filters (B1b and C1b) are used
to characterize the positive sampling artifact, namely gas phase compounds that adsorb to the quartz fiber filters. Material
5 collected on QBQ back filters can be assumed to mainly consist of adsorbed gas-phase compounds corresponding to a positive
gas-phase artefact (Cheng and He, 2015). This is confirmed by the chemical analysis of back filters in this study, which differs
considerably from that of the corresponding front filters, as detailed in Sect. S3[..¹⁰⁴]. The back filters show small mass
loadings - roughly 6 and 13 % of the masses of their respective front filters. The large mass difference between front and back
filters suggests efficient sampling of a dominant aerosol phase on front filters and a small positive sampling artifact. The front
10 filters were not corrected for the sampling artifact.

The total SOA mass concentration in the chamber derived from PTR-MS measurements was of the order of 10 µg/m³,
cf. Table 2. Overall the SMPS measured up to four times higher total mass concentrations than the PTR-MS. This difference
might be due to [..¹⁰⁵]some factors related to the individual steps of the chemical analysis, [..¹⁰⁶]e.g. filter sampling, extraction
from the filter and analysis by PTR-MS. An earlier study using an impactor-based thermal-desorption PTR-MS concluded that
15 the total aerosol mass measured was typically 20 % lower than the total aerosol mass measured with an SMPS (Holzinger
et al., 2010b). The authors estimated conservatively that their PTR-MS setup detected 55-80 % of the total aerosol mass.
Filter sampling losses of up to 10 % were attributed to negative sampling artefacts, i.e. evaporation from the filter, during
sampling times of 24 h or longer in earlier work (Subramanian et al., 2004). The maximum desorption temperature during
chemical analysis was only 350 °C and previous studies on β-pinene ozonolysis and photo-oxidation of terpenes also showed
20 significant remaining volume fractions at desorption temperatures exceeding 400 °C (Emanuelsson et al., 2013, 2014). Finally,
charring and fragmentation in the PTR-MS can additionally lower PTR-MS derived total mass concentrations. Section S4 [..¹⁰⁷
]describes these processes in more detail, as well as other aspects relevant to PTR-MS data interpretation.

Figure 3 shows ion concentration thermograms of specific compounds desorbing from front filter C1f. Table 4 complements
information in Fig. 3 and Sect. S6 [..¹⁰⁸]gives the full list of ions detected by PTR-MS from filter C1f. In Fig. 3 most ions
25 show the highest concentrations at a desorption temperature of 150 °C, in agreement with Fig. 2[..¹⁰⁹].

¹⁰³ removed: low concentrations as

¹⁰⁴ removed: in the SI

¹⁰⁵ removed: several reasons that are

¹⁰⁶ removed: i.e.

¹⁰⁷ removed: in the SI

¹⁰⁸ removed: in the SI

¹⁰⁹ removed: , but also show significant concentrations at other temperature steps.

A pure compound is expected to desorb from the filter at temperatures between its melting and boiling temperatures. Dusek et al. (2013) observed this on the same analytical setup for dicarboxylic acids. [¹¹⁰] In principle, pure compounds will be detected by the PTR-MS as an ion of similar mass and only in this temperature window. There are several possible reasons, why the same ion is observed over a range of temperatures. Since fragmentation of chemical compounds can occur during thermal desorption in the oven and ionization in the PTR-MS (see Sect. S4[¹¹¹]) a fraction of the detected ions are likely fragments of larger (heavier) compounds. This fragmentation can occur at all desorption temperatures and consequently fragments are detected over a range of temperatures. Moreover, an SOA particle usually does not consist of a single compound, but is rather a complex mixture of compounds (Cappa et al., 2008). A specific compound in this mixture will only desorb significantly, when the melting point of the mixture is reached, which might differ from the melting point of the single compound. [¹¹²] The detection of small ions that are not likely to be present in the particle phase by themselves over a wide range of desorption temperatures indicates oligomers. Recent studies show that high molecular weight dimer esters contribute significantly to SOA from the ozonolysis of α -pinene (Kristensen et al., 2016). These low volatile compounds are believed to form from gas-phase reactions of the α -pinene derived Criegee Intermediate with abundant α -pinene oxidation products such as pinic acid. Decomposition of the dimer esters such as those reported in Kristensen et al. (2016) and subsequent volatilization of the carboxylic acid moieties could at least partly explain the detection of specific ions over a range of desorption temperatures.

The relative [¹¹³] contributions of different compounds to the total SOA mass was similar on front filters, despite differences in total concentrations. For instance, the top ten ions (ranked by amount) desorbing from filter C1f at 150°C ([¹¹⁴] panel a in Fig. 3 and Table 2) can be found in nearly the same order on filters B1f, B2f and C2f (not shown). However, filters C1f and C2f show higher concentrations compared to filters B1f and B2f, see also Table 2. Different aerosol yields were reported earlier when using different OH scavengers in carbohydrate ozonolysis experiments (Docherty and Ziemann, 2003; Keywood et al., 2004). The reaction of OH with different scavengers generates different products. Consequently, the RO₂/HO₂ ratios change depending on the scavenger used, influencing the volatility distribution of products of α -pinene SOA. Overall, an increase of SOA yield is predicted when using cyclohexane as OH scavenger compared to 2-butanol (Jenkin, 2004). Assuming that 1-butanol [¹¹⁵] behaves like 2-butanol (Shilling et al., 2008), the larger desorbed aerosol mass detected by PTR-MS in the cyclohexane experiments is consistent with these considerations. However, the most abundant reaction products were not affected.

The chemical composition of aerosol found in this study was compared to previously published chemical compositions of ambient aerosol and SOA derived from α -pinene ozonolysis (in dry, dark, and low-NO_x conditions). [¹¹⁶] Panel b in Fig. 3 shows concentration thermograms of ions with masses attributed to compounds reported previously, cf. Table 4. The PTR-MS

¹¹⁰removed: Such a pure compound should in principle

¹¹¹removed: in the SI

¹¹²removed: Specifically, the

¹¹³removed: contribution of chemical compounds to

¹¹⁴removed: Panel

¹¹⁵removed: to behave

¹¹⁶removed: The chosen references (cf. Table 3) preferably listed detected constituents of particulate matter to allow direct comparison with compounds found in the present study. Preference was furthermore given to such studies that also used PTR-MS and that were investigating α -pinene ozonolysis.

allowed discrimination of particulate reaction products reported earlier (Holzinger et al., 2005, 2010a; Winterhalter et al., 2003; Jenkin, 2004; Jaoui and Kamens, 2003). In many cases the identification could be positively confirmed, but in some cases an original attribution could be falsified (details can be found in Sect. S4^[..¹¹⁷]). Some references in Table 4 and in Sect. S5 ^[..¹¹⁸] are bracketed to indicate when the assigned formulae for ion masses differed from those in the literature. Compounds predicted by modelling studies are noted by their capitalised Master Chemical Mechanism name in the description field in Table 4 and Sect. S6^[..¹¹⁹], confirming the presence of several predicted species. These compounds include pinic acid (compound #72 in Sect. S6) and pinonic acid (#116 in Sect. S6) which are also shown in Fig. 1.

Figure 4 shows the mass ^[..¹²⁰]spectra of compounds that desorbed from filter C1f at 150 °C. Most ions have a mass below 250 Da, indicating no direct observation of oligomers. However, several fragmentation patterns were detected in the data as highlighted by the arrows in Fig. 4: the light green arrow connects peaks with a mass difference of 14.016 Da (corresponding to a CH₂ group) and the dark blue arrow connects peaks with a mass difference of 18.011 Da (water). Details on fragmentation patterns can be found in Sect. S4^[..¹²¹]. Fragmentation patterns in the mass spectra ^[..¹²²] indicate that large compounds like oligomers and/or complex organic mixtures were present on the filters, as also reported in the literature (Docherty et al., 2005; Gao et al., 2004; Cappa et al., 2008; Kristensen et al., 2016) but that these compounds decompose during desorption or in the PTR-MS during ionization before they ^[..¹²³] can be detected as smaller ions.

3.2.3 O:C ratio

Figure 5 shows the measured O:C ratio versus desorption temperature for selected filters. The O:C ratio of desorbed material increases from 0.18 to 0.25 when the desorption temperature increases from 150 to 250 °C. At higher desorption temperatures the O:C ratio levels off and ^[..¹²⁴] remains constant at ca. 0.25. The O:C ratios of material desorbing from the back filters are similar to those of the front filters with averages of 0.21 (B1b) and 0.22 (C1b), cf. Table 2.

The observed increase in O:C ratio at increasing desorption temperatures (below 250 °C) is to be expected if functionalization yields oxygenated compounds with lowered volatility (Jimenez et al., 2009; Holzinger et al., 2010b). For material desorbing at temperatures above 250 °C, this correlation seems to break down and oligomerization is likely to be more important. Oligomerization reactions can be accompanied by the exclusion of water (Tolocka et al., 2004) that goes undetected in the PTR-MS, lowering O:C ratios. The desorption temperature of formed oligomers and complex mixtures is also higher than the desorption temperature of their single constituents (Cappa et al., 2008). Therefore oligomerization can decrease the volatility of compounds without raising the O:C ratios, resulting in the observed plateau of O:C ratios at high desorption temperatures.

¹¹⁷removed: in the SI). Bracketed

¹¹⁸removed: in the SI

¹¹⁹removed: in the SI

¹²⁰removed: spectrum

¹²¹removed: in the SI

¹²²removed: show indirectly

¹²³removed: were

¹²⁴removed: stays

Literature values for O:C ratios of SOA from α -pinene ozonolysis are generally [..¹²⁵] somewhat higher than the values reported here: Shilling et al. (2008) investigated SOA from α -pinene ozonolysis and report O:C ratios around 0.33 for aerosol loadings comparable to this study. Aiken et al. (2008) report O:C ratios around 0.3 for laboratory SOA from α -pinene ozonolysis and observe [..¹²⁶] more oxidized aerosol [..¹²⁷] in ambient samples. These two studies (Shilling et al., 2008; Aiken et al., 25 2008) used aerosol mass spectrometers to determine the O:C ratio, while Holzinger et al. (2010a) employed a PTR-MS, as in the present study. They report a measured O:C ratio of 0.33-0.48 for remote ambient aerosol in the Austrian alps.

PTR-MS measurements may underestimate O:C ratios because of several factors including charring and fragmentation due to ionisation, cf. Sect. S4[..¹²⁸]. Holzinger et al. (2010a) assessed in detail how oxygen loss - common in PTR-MS measurements - lowers O:C ratios. However, this was not taken into account for data reported here.

3.3 Isotopic composition

3.3.1 Total carbon and thermally desorbed material

5 Figure 6, panel a, shows the isotopic composition of total carbon on the filters relative to the isotopic composition of the precursor α -pinene. The aerosol on all front filters is enriched in carbon 13 relative to the initial α -pinene, and the enrichment is larger for filter B1f (1.2‰) than for filters C1f (0.6‰) and C2f (0.7‰). Compounds desorbing from back filter C2b, which [..¹²⁹] very likely represent gas phase material, are depleted by 0.8‰.

Panel b in Fig. 6 shows $\Delta(^{13}\text{C})$ of thermally desorbed filter material as a function of desorption temperature. Aerosol 10 on the front filters shows a ¹³C enrichment of 0.2-2.8‰ relative to the initial compound[..¹³⁰]. The most volatile fraction that desorbed at 100 °C consistently shows the highest enrichment. SOA compounds desorbing at 100 °C are enriched in ¹³C compared to 150 °C by about 0.7 to 1.9‰, cf. Table 2. The $\Delta(^{13}\text{C})$ values of SOA do not change significantly with temperature at desorption temperatures above 150 °C. SOA formed in the presence of 1-butanol (filter B1f) is enriched by an additional 0.2-1.3‰ compared to SOA formed in the presence of cyclohexane (filters C1f and C2f). The gas-phase compounds desorbing 15 at 150 °C from back filter B1b are depleted by 0.7‰ compared to the initial α -pinene and depleted by 1.9‰ with respect to the particulate SOA on filter B1f. This is expected [..¹³¹] due to isotopic mass balance. The isotopic enrichment of gas-phase compounds on filter B1b at 100 °C and 350 °C is similar to that of the corresponding particulate matter on front filter B1f. The low concentrations detected on the back filters at these desorption temperatures preclude any in-depth discussion of the enrichment seen at those temperatures.

20 Panel c in Fig. 6 shows the volume-normalized peak areas, i.e. the peak areas detected by the IR-MS divided by the total air volume sampled on the filter. This quantity allows comparison of the measured peak areas independent of sampling duration

¹²⁵removed: found to be

¹²⁶removed: in general

¹²⁷removed: (and higher O:C ratios)

¹²⁸removed: in the SI

¹²⁹removed: potentially originate from the positive gas-phase artefact

¹³⁰removed: and the

¹³¹removed: with respect to the

and should therefore be similar for filters sampling the same experiment. Indeed, the volume-normalized peak areas of the front filters are similar. As was [..¹³²]shown in the PTR-MS measurements (Fig. 2 and 3), most compounds desorb from the front filters at 150 °C. [..¹³³]Good correlation of the volume-normalized peak areas (measured by IR-MS) and the filter loadings (measured by PTR-MS) was also [..¹³⁴]seen in Dusek et al. (2013). As with the PTRMS results, the back filter shows only small peak areas over the whole temperature range. The smaller amount of carbon mass on the back filters [..¹³⁵]results in larger uncertainty [..¹³⁶]in $\Delta(^{13}\text{C})$ compared to the front filters.

$\Delta_{\text{TC}}(^{13}\text{C})$ values are close to $\Delta(^{13}\text{C})$ values at 150 °C (Fig. 6 and Table 2). $\Delta_{\text{TC}}(^{13}\text{C})$ values represent a convolution of the volume-normalised peak area and $\Delta(^{13}\text{C})$, with a dominant contribution of $\Delta(^{13}\text{C})$ [..¹³⁷]at 150 °C. Total carbon analysis however misses details like the enrichment of the most volatile mass fraction desorbing at 100 °C.

3.3.2 Can position-specific isotope analysis of α -pinene explain the enriched aerosol phase?

Table 1 lists $\Delta_i(^{13}\text{C})$ for each C-atom of all analysed α -pinene samples. Single sites show variations between -6.9% and 10.5% . The α -pinene samples from manufacturers Sigma-Aldrich, Acros Organics and Merck have similar position-specific isotope profiles. It is likely that [..¹³⁸]these three manufacturers sell α -pinene [..¹³⁹]with the same origin (e.g. natural) and use similar preparation techniques. The last sample (from Alfa Aesar) has a slightly different profile which [..¹⁴⁰]would seem to indicate a different origin and/or purification method. [..¹⁴¹] α -pinene samples [..¹⁴²]from Acros Organics ($j = 3$) and Merck ($j = 4$) have similar $\Delta_i(^{13}\text{C})$ profiles but differ by 1.1 ‰ in their bulk value.

Unfortunately, PSIA could not be performed on the α -pinene used in chamber experiments (it was used up and is [..¹⁴³]no longer available from the manufacturer [..¹⁴⁴]). The α -pinene used in chamber experiments has a bulk isotopic composition of $\delta_{\text{TC}}^{13}\text{C} = (-29.96 \pm 0.08) \%$ which differs by up to 3 ‰ from the other α -pinene samples, cf. Table 1. Given that the bulk isotopic composition is [..¹⁴⁵]not correlated with the position-specific isotope profiles and assuming that the manufacturer did not change product origin or purification method, it is probable that the two α -pinene samples from Sigma-Aldrich share similar position-specific isotope profiles. It is therefore assumed for the remainder of the discussion that the α -pinene used for the SOA experiments has the same position-specific isotope profile as the batch from Sigma-Aldrich on which PSIA was performed. The $\Delta_i(^{13}\text{C})$ distribution of that sample is visualised in Fig. 7.

¹³²removed: already shown from

¹³³removed: The good

¹³⁴removed: shown by Dusek et al. (2013). Also similar to

¹³⁵removed: result

¹³⁶removed: of

¹³⁷removed: from

¹³⁸removed: those

¹³⁹removed: from

¹⁴⁰removed: could tentatively be explained by the source material

¹⁴¹removed: The data in Table 1 indicates that the position-specific isotope profiles of different

¹⁴²removed: is independent of the bulk (total carbon) enrichment, $\delta_{\text{TC}}^{\text{C}j} (^{13}\text{C})$, of that sample: α -pinene samples

¹⁴³removed: not

¹⁴⁴removed: anymore

¹⁴⁵removed: no indicator for differing

[..¹⁴⁶] Here a limiting case is presented for the isotopic difference of a number of plausible oxidation products. The underlying assumptions exclude isotope dependent changes in product branching ratios, as well as effects of temperature, relative humidity, pressure, ozone concentration, etc. This simplistic approach allows to estimate the maximum isotopic enrichment in α -pinene [..¹⁴⁷] fragments using the $\Delta_i(^{13}\text{C})$ profiles obtained from PSIA. Table 5 shows predicted maximal enrichments/depletions if a single carbon atom or reasonable combinations of three carbon atoms are split off the parent compound [..¹⁴⁸]. Based on the chemical reaction pathways presented in Fig. 1, volatile reaction products such as acetone, CO, and formaldehyde can [..¹⁴⁹] reasonably be assigned to specific sites in the parent α -pinene. The minor (potentially gaseous) expelled fragment is predicted to have an overall isotopic difference relative to the initial α -pinene, $\Delta_{\text{gas}}(^{13}\text{C})$, similar to the measured $\Delta_i(^{13}\text{C})$ value for the carbon atom's former position as seen in Fig. 7. The larger fragment, which would partition to the aerosol phase, is predicted to have an overall $\Delta_{\text{aerosol}}(^{13}\text{C})$ value equal to the average of the $\Delta_i(^{13}\text{C})$ values of the remaining C atoms. For example, the pathway leading to formaldehyde in the sixth box in Fig. 1 is predicted to deplete formaldehyde by $\Delta_9(^{13}\text{C}) = 6.7\%$ relative to the initial compound and leave the corresponding major fragment (denoted as 'R' in Fig. 1) enriched by $[\Delta_i(^{13}\text{C})]_{\text{av}(i=1-8,10)} = 0.8\%$. Here, $[\dots]_{\text{av}(i=1-8,10)}$ denotes the mean of $\Delta_i(^{13}\text{C})$ values for C atoms 1-8 and 10. Expelled C-atoms from positions with small $\Delta_i(^{13}\text{C})$ values, e.g. C₇, will only have a small impact on the isotopic composition of the remaining fragment. For expulsion of C₂, a depletion of -1.1% is predicted for the aerosol fragment relative to the initial α -pinene.

If three carbon atoms are expelled, as in the case of acetone, the [..¹⁵⁰] enrichment of the minor fragment relative to the initial α -pinene is calculated as the average of the $\Delta_i(^{13}\text{C})$ values of the respective expelled positions C₈, C₁, C₉ or C₁₀, C₁, C₉, see Fig. 1. The formation of acetone [..¹⁵¹] may involve methyl migration of either the C₈ or C₁₀ atom. The gaseous fragments composed of three carbon atoms are predicted to show $\Delta_{\text{gas}}(^{13}\text{C})$ values of -0.7% and -2.0% and the corresponding $\Delta_{\text{aerosol}}(^{13}\text{C})$ values for the larger fragment are 0.4% and 1.0%, cf. Table 5. These calculations are based on the measured position-specific enrichment for sample 2 in Table 1, but the results and conclusions drawn do not change significantly when performing similar calculations for the other α -pinene samples where PSIA data is available.

4 Discussion

In this experiment we have run α -pinene ozonolysis to completion and analysed the SOA and some of the gas phase material. We argue that the observed isotopic abundancies are largely due to a combination of isotope-dependent changes in product branching ratios and unequal partitioning of carbon atoms from specific sites in α -pinene into the aerosol

¹⁴⁶removed: Some simple considerations regarding the maximum expected isotopic enrichment of

¹⁴⁷removed: fragmentation products can be performed based on

¹⁴⁸removed: , based on the simple assumptions that such reactions run to completion and that other competing reactions (branching indicated by arrows in Fig. 1) have no effect on the isotopic enrichment.

¹⁴⁹removed: in most cases be assigned as originating from specific sites of

¹⁵⁰removed: isotopic difference

¹⁵¹removed: involves

and gas phases. Additional effects could include isotope dependent variations in partitioning of semi-volatile compounds between the gas and condensed phases.

- 20 The observed [¹⁵²] ¹³C enrichment in compounds from the front filters [¹⁵³](SOA) and the depletion in compounds from the back [¹⁵⁴] filters (gas phase) are generally larger or [¹⁵⁵] equal in magnitude to those predicted by position-specific isotope effect analysis (cf. Table 5). [¹⁵⁶] The data shown in Table 5 are limiting values and show that PSIA is capable, in principle, of producing abundancies of similar magnitude to what was observed in our experiment. This mechanism does not include concomitant enrichment due to isotope effects on product branching ratios.
- 25 [¹⁵⁷] The other explanations include isotope-dependent changes in branching ratios in the reaction mechanism (Fig. 1) and incomplete reactions. [¹⁵⁸] It has been shown previously in simple systems (e.g. evaporation of solvents and sorption of vanillin) that each carbon position can have its own isotopic fractionation and that different positions can show [¹⁵⁹] opposing isotope effects at the same time (Höhener et al., 2012; Julien et al., 2015). In chemical reactions, the substitution of a ¹²C atom by ¹³C will affect isomerisation and stabilisation dynamics by changing vibrational frequencies with an associated change in zero point energies. Therefore, positions that are not reaction sites can also show isotope effects, which have been termed non-covalent isotope effects (Wade, 1999), as has been observed during the chain-shortening reaction for the bioconversion of
- 5 ferulic acid to vanillin (Botosoa et al., 2009b). It is generally difficult to predict which position has which isotope effect, but it has been shown that isotopic substitution in ring structures at positions that carry functional groups [¹⁶⁰] lead to stronger position-specific isotope effects compared to positions that have no functional groups attached (Höhener et al., 2012; Botosoa et al., 2009b). Similarly, the C-atoms in α -pinene that are not part of the ring structure might have large position-specific isotope effects. [¹⁶¹] Höhener et al. (2012) note that for vanillin, as we also show in Table 5 [¹⁶²], such effects [¹⁶³]
- 10 5 [¹⁶⁴]

¹⁵²removed: enrichment of aerosol compounds desorbing

¹⁵³removed: as well as the observed depletion of gas-phase compounds desorbing

¹⁵⁴removed: filter

¹⁵⁵removed: of similar magnitude compared to the predicted

¹⁵⁶removed: Given the assumptions behind the position-specific isotope effects predicted in table 5 (i.e. only one fragmentation reaction is considered out of many with potentially opposing effects on isotopes, and that reaction proceeds to completeness) the results do not prove that the simple position-specific isotope effects considered here were the leading cause for the observed enrichment in the particle phase.

¹⁵⁷removed: A more realistic set of possible explanations for the observed fractionation of SOA relative to α -pinene should

¹⁵⁸removed: These effects complicate the analysis significantly as new factors come into play, including most notably, kinetically-derived position-dependent isotopic fractionation.

¹⁵⁹removed: normal and inverse

¹⁶⁰removed: leads

¹⁶¹removed: However as Höhener et al. (2012) note for the case of vanillin, and

¹⁶²removed: in a simplified scenario

¹⁶³removed: leave the bulk isotopic composition largely unchanged, making the use of PSIA in SOA studies beyond what has been done here potentially challenging.

¹⁶⁴removed: Discussion

[..¹⁶⁵] can produce large fractionations in the small fragments and small fractionations in the large. Accordingly, in α -pinene [..¹⁶⁶] there is about an order of magnitude difference between the site-dependent enrichments seen in the C₁₀ molecule, 6 – 10‰, and the enrichments seen in the SOA, 0.6 – 1.2‰.

[..¹⁶⁷] Kinetic isotope effects associated with fragmentation provide a [..¹⁶⁸] possible explanation for the enrichment of the particle phase with respect to the gas phase. After the first two reaction steps (i.e. formation of the Criegee intermediate and subsequent decomposition/stabilisation/isomerization of it, cf. Fig. 1) [..¹⁶⁹] the products will be distributed between the gas and particle [..¹⁷⁰] phases according to their [..¹⁷¹] respective partitioning coefficients. This partitioning is not expected to lead to significant isotopic fractionation [..¹⁷²] within a chemical species. A number of these products are small [..¹⁷³] volatile compounds that partition to the gas phase. [..¹⁷⁴] The remaining particle phase [..¹⁷⁵] would be enriched consistent with observations reported previously (Aggarwal and Kawamura, 2008; Kirillova et al., 2013, 2014). Fragmentation followed by functionalization is expected to be accompanied by elevated O:C ratios in both [..¹⁷⁶] products as detailed in the introduction. This is in line with the observed increasing O:C ratios of desorbed material from front filters at increasing desorption temperatures below 250 °C (Fig. 5), and with O:C ratios that are generally elevated for back filter material desorbing at all temperatures (Table 2).

Large equilibrium fractionation due to gas-particle partitioning could also explain the observations given that individual compounds might show isotope effects of 1 – 2‰ due to partial volatilisation. In an ensemble of compounds, however, most individual compounds are likely to be found predominantly in one phase; only a fraction of products have intermediate volatilities. In the case of α -pinene ozonolysis shown in Fig. 1 small first generation products like CO, HCHO and acetone will be gaseous and the larger entities including prominent acids will [..¹⁷⁷] partition to particles due to their lower vapour pressure. Ongoing reactions (e.g. dimer formation and oligomerization) will lower their vapour pressure even further. Equilibrium isotope effects of single compounds are therefore diluted and hence less likely to cause the observed isotopic enrichment in SOA.

¹⁶⁵removed: SOA formation

¹⁶⁶removed: ozonolysis includes several chemical processes that influence the isotopic compositions of product species. The presented data does not allow quantification of the roles of the processes that lead to enrichment of the aerosol phase with respect to the gas phase and this section discusses different possibilities to explain the observations

¹⁶⁷removed: Isotope

¹⁶⁸removed: likely

¹⁶⁹removed: all compounds are distributed between

¹⁷⁰removed: phase

¹⁷¹removed: partitioning coefficient

¹⁷²removed: . Some of the possible next reaction steps are fragmentation reactions, that (if not complete) lead to a number of reaction products that are depleted with respect to the initial compounds. A part

¹⁷³removed: and

¹⁷⁴removed: This leads to a net loss of material from the particle phase. Therefore the

¹⁷⁵removed: will overall

¹⁷⁶removed: fragments

¹⁷⁷removed: be on the

[..¹⁷⁸][..¹⁷⁹]

10 The present study allows [..¹⁸⁰]new insight on observations of isotopically enriched [..¹⁸¹]ambient SOA. In some cases isotopic enrichment in ambient aerosol was attributed to photochemical ageing during long-range transport (Kirillova et al., 2013; Pavuluri et al., 2011). However, Fu et al. (2012) note that a normal kinetic isotope effect cannot explain their observation of aerosol that was even more enriched than aerosol from biomass burning. The authors noted that such aerosol occurred predominantly during [..¹⁸²]the day during episodes of high abundance of biogenic SOA. The [..¹⁸³]present study suggests
15 that the site-specific distribution of ¹³C in the source material itself governs the abundance of ¹³C [..¹⁸⁴]in SOA.

5 Conclusions

The isotopic and chemical compositions of SOA generated from [..¹⁸⁵]dark ozonolysis of α -pinene were determined using isotope ratio mass spectrometry and thermal-desorption [..¹⁸⁶]PTR-MS, and PSIA was applied for the first time on α -pinene from [..¹⁸⁷]a series of manufacturers. A key result is the first observations of strong site dependent enrichments
20 and depletions in ¹³C in α -pinene, with values between -6.9‰ and $+10.5\text{‰}$ relative to the bulk composition. Total carbon from SOA collected on front filters was enriched in ¹³C by $0.6 - 1.2\text{‰}$ with respect to the initial α -pinene precursor. Total carbon adsorbed on the back filters, designed to sample gas-phase compounds, was depleted by -0.8‰ .

High-resolution data retrieved by a PTR-MS [..¹⁸⁸]detected more than 400 ions. More than 90 % of the total desorbed mass as measured by PTR-MS (from front filters) was [..¹⁸⁹]unambiguously identified and discussed in the context of the current

¹⁷⁸removed: The reason behind the enrichment in material desorbing from front filters at 100 °C cannot be unambiguously identified. The chemical analysis did not allow to identify single compounds or groups of compounds that contributed significantly more to the total aerosol concentration at 100 °C than at 150 °C and therefore could lead to the observed enrichment. Isotope effects associated with sampling artefacts, which are generally not well known, provide room for speculation on how to interpret the enrichment at 100 °C. During the negative sampling artefact, isotopically light isotopologues re-volatilise from the ensemble of sampled compounds preferentially leading to an overall isotopic enrichment in compounds that are left on the filter. Re-volatilisation should have it's largest effect at 100 °C. Another explanation can be based on oligomerisation. Hall and Johnston (2012) observed significant evaporation of oligomers in a thermodesorber already at desorption temperatures below 100 °C. The effect of oligomerisation on isotopes is not known, but if it leads to enrichment, the fragments of decomposed oligomers could be enriched and explain the observed enrichment in the particle phase. On the contrary, fragments of oligomers make up a large fraction of compounds that desorb at temperatures above 150

¹⁷⁹removed: as suggested by the PTR-MS data. Stable $\Delta(^{13}\text{C})$ values at these desorption temperatures suggest that oligomerization does not influence the isotopic composition significantly. It further seems that oligomerization of already enriched oxidation products conserves the $\Delta(^{13}\text{C})$ value. Overall the role of oligomerisation on the isotope budget remains unclear, leaving room for further studies.

¹⁸⁰removed: linking ambient

¹⁸¹removed: aerosol to SOA generated from α -pinene in the laboratory

¹⁸²removed: daytimes

¹⁸³removed: results in the present study suggest that different effects have to be taken into account as they provide an additional way of enriching SOA in

¹⁸⁴removed: . The origin of the observed enrichment is clearly an interesting subject for continued research.

¹⁸⁵removed: the

¹⁸⁶removed: techniques and related to each other.

¹⁸⁷removed: different manufacturers. The results showed strong enrichments for specific C-atoms,

¹⁸⁸removed: allowed for detection of

¹⁸⁹removed: identified by chemical formulas, unambiguously ,

literature. [..¹⁹⁰] SOA mainly desorbed from the filters at 150 °C [..¹⁹¹], and larger compounds likely formed in oligomerization reactions decomposed during extraction or ionisation. Besides the fragments from such oligomers, single constituents of complex organic mixtures formed on the filter were also detected as single ions of lower mass which show significant non-zero concentrations at desorption temperatures higher than 150 °C. The observed constant O:C ratio at desorption temperatures exceeding 250 °C also indicate fragments of larger molecules. At lower temperatures the O:C ratio increases from 0.18 to 0.25 indicating functionalization reactions during SOA formation.

[..¹⁹²] Analysis of the isotopic composition as a function of desorption temperature showed that the isotopic composition of material desorbing at 150 °C was similar to the isotopic composition of total carbon. [..¹⁹³] Functionalization typically follows fragmentation in monoterpene ozonolysis and was shown to drive the O:C temperature profiles. [..¹⁹⁴] Many variables including product branching ratios, temperature, pressure, humidity, OH, NO_x, etc. can in principle have an effect on the isotopic abundance of ¹³C in SOA and leave room for further studies. The present study suggests that the site-specific distribution of ¹³C in the source material itself governs the abundance of ¹³C in SOA.

Acknowledgements. The authors thank IntraMIF and the University of Copenhagen for supporting this research. The research has received funding from the European Community's Seventh Framework Programme (FP7/2007-2013) under grant agreement number 237890. The thermogram ¹³C analysis was funded by The Netherlands Organisation for Scientific Research (NWO), grant number 820.01.001.

¹⁹⁰removed: Generated

¹⁹¹removed: from the filters, but

¹⁹²removed: Total carbon from SOA collected on front filters was enriched in ¹³C by 0.6 – 1.2‰ with respect to the initial α -pinene precursor. Total carbon adsorbed on the back filters, which supposedly originates from adsorption of gas-phase compounds to the filter was depleted by –0.8‰.

¹⁹³removed: A potential bulk isotopic signature on the formed SOA based on the PSIA results becomes less pronounced even when a simple fragmentation reaction in which a moiety of three carbon atoms is split off is assumed to go to completion. Such simple fragmentation reactions are not likely to explain the observed enrichment of the aerosol compounds and depletion of the gas-phase compounds but can also not be ignored. Incomplete fragmentation yielding small, isotopically light compounds can also cause the observed enrichment in the particle phase and depletion in the gas-phase, independent of position-specific enrichment.

¹⁹⁴removed: However, the isotopic depletion in reaction products associated with functionalization reactions does not seem to play a large role in the overall isotopic signature. Other factors including the effect of isotopic substitution on volatility and potential isotopic fractionation due to oligomerisation cannot be ruled out either. The observed enrichment and its underlying reasons are potentially important for interpreting isotopic compositions of ambient aerosol

References

- Aggarwal, S. G. and Kawamura, K.: Molecular distributions and stable carbon isotopic compositions of dicarboxylic acids and related compounds in aerosols from Sapporo, Japan: Implications for photochemical aging during long-range atmospheric transport, *J. Geophys. Res. Atmos.*, 113, D14 301, doi:10.1029/2007JD009365, 2008.
- Aiken, A. C., DeCarlo, P. F., Kroll, J. H., Worsnop, D. R., Huffman, J. A., Docherty, K. S., Ulbrich, I. M., Mohr, C., Kimmel, J. R., Sueper, D., Sun, Y., Zhang, Q., Trimborn, A., Northway, M., Ziemann, P. J., Canagaratna, M. R., Onasch, T. B., Alfarra, M. R., Prevot, A. S. H., Dommen, J., Duplissy, J., Metzger, A., Baltensperger, U., and Jimenez, J. L.: O/C and OM/OC Ratios of Primary, Secondary, and Ambient Organic Aerosols with High-Resolution Time-of-Flight Aerosol Mass Spectrometry, *Environ. Sci. Technol.*, 42, 4478–4485, doi:10.1021/es703009q, 2008.
- Andreae, M. O. and Crutzen, P. J.: Atmospheric Aerosols: Biogeochemical Sources and Role in Atmospheric Chemistry, *Science*, 276, 1052–1058, doi:10.1126/science.276.5315.1052, 1997.
- Bayle, K., Akoka, S., Remaud, G. S., and Robins, R. J.: Non-Statistical ^{13}C Distribution during Carbon Transfer from Glucose to Ethanol During Fermentation is Determined by the Catabolic Pathway Exploited, *J. Biol. Chem.*, doi:10.1074/jbc.M114.621441, 2014a.
- Bayle, K., Gilbert, A., Julien, M., Yamada, K., Silvestre, V., Robins, R. J., Akoka, S., Yoshida, N., and Remaud, G. S.: Conditions to obtain precise and true measurements of the intramolecular ^{13}C distribution in organic molecules by isotopic ^{13}C nuclear magnetic resonance spectrometry, *Anal. Chim. Acta.*, 846, 1–7, doi:10.1016/j.aca.2014.07.018, 2014b.
- Botosoa, E. P., Caytan, E., Silvestre, V., Robins, R. J., Akoka, S., and Remaud, G. S.: Unexpected Fractionation in Site-Specific ^{13}C Isotopic Distribution Detected by Quantitative ^{13}C NMR at Natural Abundance, *J. Am. Chem. Soc.*, 130, 414–415, doi:10.1021/ja0771181, 2008.
- Botosoa, E. P., Blumenstein, C., MacKenzie, D. A., Silvestre, V., Remaud, G. S., Kwiecień, R. A., and Robins, R. J.: Quantitative isotopic ^{13}C nuclear magnetic resonance at natural abundance to probe enzyme reaction mechanisms via site-specific isotope fractionation: The case of the chain-shortening reaction for the bioconversion of ferulic acid to vanillin, *Anal. Biochem.*, 393, 182–188, doi:10.1016/j.ab.2009.06.031, 2009a.
- Botosoa, E. P., Silvestre, V., Robins, R. J., Rojas, J. M. M., Guillou, C., and Remaud, G. S.: Evidence of ^{13}C non-covalent isotope effects obtained by quantitative ^{13}C nuclear magnetic resonance spectroscopy at natural abundance during normal phase liquid chromatography, *J. Chromatogr. A*, 1216, 7043–7048, doi:10.1016/j.chroma.2009.08.066, 2009b.
- Brooks, P. D., Geilmann, H., Werner, R. A., and Brand, W. A.: Improved precision of coupled d^{13}C and d^{15}N measurements from single samples using an elemental analyzer/isotope ratio mass spectrometer combination with a post-column six-port valve and selective CO_2 trapping; improved halide robustness of the combustion reactor using CeO_2 , *Rapid Commun. Mass Sp.*, 17, 1924–1926, doi:10.1002/rcm.1134, 2003.
- Camredon, M., Hamilton, J. F., Alam, M. S., Wyche, K. P., Carr, T., White, I. R., Monks, P. S., Rickard, A. R., and Bloss, W. J.: Distribution of gaseous and particulate organic composition during dark alpha-pinene ozonolysis, *Atmos. Chem. Phys.*, 10, 2893–2917, doi:10.5194/acp-10-2893-2010, 2010.
- Cappa, C. D., Lovejoy, E. R., and Ravishankara, A. R.: Evidence for liquid-like and nonideal behavior of a mixture of organic aerosol components, *P. Natl. Acad. Sci. USA*, 105, 18 687–18 691, doi:10.1073/pnas.0802144105, 2008.
- Ceburnis, D., Garbaras, A., Szidat, S., Rinaldi, M., Fahrni, S., Perron, N., Wacker, L., Leinert, S., Remeikis, V., Facchini, M. C., Prevot, A. S. H., Jennings, S. G., Ramonet, M., and O’Dowd, C. D.: Quantification of the carbonaceous matter origin in submicron marine aerosol by ^{13}C and ^{14}C isotope analysis, *Atmos. Chem. Phys.*, 11, 8593–8606, doi:10.5194/acp-11-8593-2011, 2011.

- Chacon-Madrid, H. J. and Donahue, N. M.: Fragmentation vs. functionalization: chemical aging and organic aerosol formation, *Atmos. Chem. Phys.*, 11, 10553–10563, doi:10.5194/acp-11-10553-2011, 2011.
- 5 Cheng, Y. and He, K.: Uncertainties in observational data on organic aerosol: An annual perspective of sampling artifacts in Beijing, China, *Environ. Pollut.*, 206, 113–121, doi:10.1016/j.envpol.2015.06.012, 2015.
- Coplen, T. B.: Guidelines and recommended terms for expression of stable-isotope-ratio and gas-ratio measurement results, *Rapid Commun. Mass Sp.*, 25, 2538–2560, doi:10.1002/rcm.5129, 2011.
- Coplen, T. B., Brand, W. A., Gehre, M., Gröning, M., Meijer, H. A. J., Toman, B., and Verkouteren, R. M.: New Guidelines for $\delta^{13}\text{C}$ Measurements, *Anal. Chem.*, 78, 2439–2441, doi:10.1021/ac052027c, 2006.
- 5 Docherty, K. S. and Ziemann, P. J.: Effects of Stabilized Criegee Intermediate and OH Radical Scavengers on Aerosol Formation from Reactions of beta-Pinene with O₃, *Aerosol Sci. Tech.*, 37, 877–891, doi:10.1080/02786820300930, 2003.
- Docherty, K. S., Wu, W., Lim, Y. B., and Ziemann, P. J.: Contributions of Organic Peroxides to Secondary Aerosol Formed from Reactions of Monoterpenes with O₃, *Environ. Sci. Technol.*, 39, 4049–4059, doi:10.1021/es050228s, 2005.
- Dockery, D. W., Pope, C. A., Xu, X., Spengler, J. D., Ware, J. H., Fay, M. E., Ferris, B. G., and Speizer, F. E.: An Association between Air
10 Pollution and Mortality in Six U.S. Cities, *New Engl. J. Med.*, 329, 1753–1759, doi:10.1056/NEJM199312093292401, 1993.
- Donahue, N. M., Robinson, A. L., Stanier, C. O., and Pandis, S. N.: Coupled Partitioning, Dilution, and Chemical Aging of Semivolatile Organics, *Environ. Sci. Technol.*, 40, 2635–2643, doi:10.1021/es052297c, 2006.
- Donahue, N. M., Epstein, S. A., Pandis, S. N., and Robinson, A. L.: A two-dimensional volatility basis set: 1. organic-aerosol mixing thermodynamics, *Atmos. Chem. Phys.*, 11, 3303–3318, doi:10.5194/acp-11-3303-2011, 2011.
- 15 Dusek, U., Meusinger, C., Oyama, B., Ramon, W., de Wilde, P., Holzinger, R., and Röckmann, T.: A thermal desorption system for measuring $\delta^{13}\text{C}$ ratios on organic aerosol, *J. Aerosol Sci.*, 66, 72–82, doi:10.1016/j.jaerosci.2013.08.005, 2013.
- Emanuelsson, E. U., Watne, A. K., Lutz, A., Ljungstrom, E., and Hallquist, M.: Influence of Humidity, Temperature, and Radicals on the Formation and Thermal Properties of Secondary Organic Aerosol (SOA) from Ozonolysis of beta-Pinene, *J. Phys. Chem. A*, 117, 10346–10358, doi:10.1021/jp4010218, 2013.
- 20 Emanuelsson, E. U., Mentel, T. F., Watne, A. K., Spindler, C., Bohn, B., Brauers, T., Dorn, H.-P., Hallquist, A. M., Haseler, R., Kiendler-Scharr, A., Müller, K.-P., Pleijel, H., Rohrer, F., Rubach, F., Schlosser, E., Tillmann, R., and Hallquist, M.: Parameterization of Thermal Properties of Aging Secondary Organic Aerosol Produced by Photo-Oxidation of Selected Terpene Mixtures, *Environ. Sci. Technol.*, 48, 6168–6176, doi:10.1021/es405412p, 2014.
- Fisseha, R., Saurer, M., Jäggi, M., Siegwolf, R. T. W., Dommen, J., Szidat, S., Samburova, V., and Baltensperger, U.: Determination of
25 primary and secondary sources of organic acids and carbonaceous aerosols using stable carbon isotopes, *Atmos. Environ.*, 43, 431–437, doi:10.1016/j.atmosenv.2008.08.041, 2009.
- Fu, P. Q., Kawamura, K., Chen, J., Li, J., Sun, Y. L., Liu, Y., Tachibana, E., Aggarwal, S. G., Okuzawa, K., Tanimoto, H., Kanaya, Y., and Wang, Z. F.: Diurnal variations of organic molecular tracers and stable carbon isotopic composition in atmospheric aerosols over Mt. Tai in the North China Plain: an influence of biomass burning, *Atmos. Chem. Phys.*, 12, 8359–8375, doi:10.5194/acp-12-8359-2012, 2012.
- 30 Gao, S., Ng, N. L., Keywood, M., Varutbangkul, V., Bahreini, R., Nenes, A., He, J., Yoo, K. Y., Beauchamp, J. L., Hodyss, R. P., Flagan, R. C., and Seinfeld, J. H.: Particle Phase Acidity and Oligomer Formation in Secondary Organic Aerosol, *Environ. Sci. Technol.*, 38, 6582–6589, doi:10.1021/es049125k, 2004.

- Gensch, I., Laumer, W., Stein, O., Kammer, B., Hohaus, T., Saathoff, H., Wegener, R., Wahner, A., and Kiendler-Scharr, A.: Temperature dependence of the kinetic isotope effect in beta-pinene ozonolysis, *J. Geophys. Res.*, 116, D20301, doi:201110.1029/2011JD016084, 2011.
- Gilbert, A., Silvestre, V., Segebarth, N., Tcherkez, G., Guillou, C., Robins, R. J., Akoka, S., and Remaud, G. S.: The intramolecular ¹³C-distribution in ethanol reveals the influence of the CO₂-fixation pathway and environmental conditions on the site-specific ¹³C variation in glucose, *Plant Cell Environ.*, 34, 1104–1112, doi:10.1111/j.1365-3040.2011.02308.x, 2011.
- Gilbert, A., Hattori, R., Silvestre, V., Wasano, N., Akoka, S., Hirano, S., Yamada, K., Yoshida, N., and Remaud, G. S.: Comparison of IRMS and NMR spectrometry for the determination of intramolecular ¹³C isotope composition: Application to ethanol, *Talanta*, 99, 1035–1039, doi:10.1016/j.talanta.2012.05.023, 2012.
- 5 Hall, W.A., and Johnston, M.V., The Thermal-Stability of Oligomers in Alpha-Pinene Secondary Organic Aerosol, *Aerosol Sci. Tech.*, 46, 983–989. doi:10.1080/02786826.2012.685114, 2012.
- Hallquist, M., Wenger, J. C., Baltensperger, U., Rudich, Y., Simpson, D., Claeys, M., Dommen, J., Donahue, N. M., George, C., and Goldstein, A. H.: The formation, properties and impact of secondary organic aerosol: current and emerging issues, *Atmos. Chem. Phys.*, 9, 5155–5236, doi:10.5194/acp-9-5155-2009, 2009.
- 10 Ho, K., Lee, S., Cao, J., Li, Y., Chow, J., Watson, J., and Fung, K.: Variability of organic and elemental carbon, water soluble organic carbon, and isotopes in Hong Kong, *Atmos. Chem. Phys.*, 6, 4569–4576, doi:10.5194/acp-6-4569-2006, 2006.
- Holzinger, R.: PTRwid: A new widget tool for processing PTR-TOF-MS data, *Atmos. Meas. Tech.*, 8, 3903–3922, doi:10.5194/amt-8-3903-2015, 2015.
- Holzinger, R., Lee, A., Paw, K. T., and Goldstein, U. A. H.: Observations of oxidation products above a forest imply biogenic emissions of very reactive compounds, *Atmos. Chem. Phys.*, 5, 67–75, doi:10.5194/acp-5-67-2005, 2005.
- Holzinger, R., Kasper-Giebl, A., Staudinger, M., Schauer, G., and Röckmann, T.: Analysis of the chemical composition of organic aerosol at the Mt. Sonnblick observatory using a novel high mass resolution thermal-desorption proton-transfer-reaction mass-spectrometer (hr-TD-PTR-MS), *Atmos. Chem. Phys.*, 10, 10 111–10 128, doi:10.5194/acp-10-10111-2010, 2010a.
- Holzinger, R., Williams, J., Herrmann, F., Lelieveld, J., Donahue, N. M., and Röckmann, T.: Aerosol analysis using a Thermal-Desorption Proton-Transfer-Reaction Mass Spectrometer (TD-PTR-MS): a new approach to study processing of organic aerosols, *Atmos. Chem. Phys.*, 10, 2257–2267, doi:10.5194/acp-10-2257-2010, 2010b.
- 20 Holzinger, R., Goldstein, A. H., Hayes, P. L., Jimenez, J. L., and Timkovsky, J.: Chemical evolution of organic aerosol in Los Angeles during the CalNex 2010 study, *Atmos. Chem. Phys.*, 13, 10 125–10 141, doi:10.5194/acp-13-10125-2013, 2013.
- Huang, L., Brook, J., Zhang, W., Li, S., Graham, L., Ernst, D., Chivulescu, A., and Lu, G.: Stable isotope measurements of carbon fractions (OC/EC) in airborne particulate: A new dimension for source characterization and apportionment, *Atmos. Environ.*, 40, 2690–2705, doi:10.1016/j.atmosenv.2005.11.062, 2006.
- Hänninen, O. O., Alm, S., Katsouyanni, K., Künzli, N., Maroni, M., Nieuwenhuijsen, M. J., Saarela, K., Srám, R. J., Zmirou, D., and Jantunen, M. J.: The EXPOLIS study: implications for exposure research and environmental policy in Europe, *J. Expo. Sci. Env. Epid.*, 14, 440–456, doi:10.1038/sj.jea.7500342, 2004.
- 30 Höhener, P., Silvestre, V., Lefrançois, A., Loquet, D., Botosoa, E. P., Robins, R. J., and Remaud, G. S.: Analytical model for site-specific isotope fractionation in ¹³C during sorption: Determination by isotopic ¹³C NMR spectrometry with vanillin as model compound, *Chemosphere*, 87, 445–452, doi:10.1016/j.chemosphere.2011.12.023, 2012.

- Iannone, R., Koppmann, R., and Rudolph, J.: Stable carbon kinetic isotope effects for the production of methacrolein and methyl vinyl ketone from the gas-phase reactions of isoprene with ozone and hydroxyl radicals, *Atmos. Environ.*, 44, 4135–4141, doi:10.1016/j.atmosenv.2010.07.046, 2010.
- Irei, S., Rudolph, J., Huang, L., Auld, J., and Hastie, D.: Stable carbon isotope ratio of secondary particulate organic matter formed by photooxidation of toluene in indoor smog chamber, *Atmos. Environ.*, 45, 856–862, doi:10.1016/j.atmosenv.2010.11.021, 2011.
- Irei, S., Takami, A., Hayashi, M., Sadanaga, Y., Hara, K., Kaneyasu, N., Sato, K., Arakaki, T., Hatakeyama, S., Bandow, H., Hikida, T., and Shimono, A.: Transboundary Secondary Organic Aerosol in Western Japan Indicated by the $\delta^{13}\text{C}$ of Water-Soluble Organic Carbon and the m/z 44 Signal in Organic Aerosol Mass Spectra, *Environ. Sci. Technol.*, 48, 6273–6281, doi:10.1021/es405362y, 2014.
- 5 Jaoui, M. and Kamens, R. M.: Gaseous and Particulate Oxidation Products Analysis of a Mixture of α -pinene + β -pinene/O₃/Air in the Absence of Light and α -pinene + β -pinene/NO_x/Air in the Presence of Natural Sunlight, *J. Atmos. Chem.*, 44, 259–297, doi:10.1023/A:1022977427523, 2003.
- Jenkin, M. E.: Modelling the formation and composition of secondary organic aerosol from alpha- and beta-pinene ozonolysis using MCM v3, *Atmos. Chem. Phys.*, 4, 1741–1757, doi:10.5194/acp-4-1741-2004, 2004.
- 10 Jimenez, J. L., Canagaratna, M. R., Donahue, N. M., Prevot, A. S. H., Zhang, Q., Kroll, J. H., DeCarlo, P. F., Allan, J. D., Coe, H., Ng, N. L., Aiken, A. C., Docherty, K. S., Ulbrich, I. M., Grieshop, A. P., Robinson, A. L., Duplissy, J., Smith, J. D., Wilson, K. R., Lanz, V. A., Hueglin, C., Sun, Y. L., Tian, J., Laaksonen, A., Raatikainen, T., Rautiainen, J., Vaattovaara, P., Ehn, M., Kulmala, M., Tomlinson, J. M., Collins, D. R., Cubison, M. J., E, Dunlea, J., Huffman, J. A., Onasch, T. B., Alfarra, M. R., Williams, P. I., Bower, K., Kondo, Y., Schneider, J., Drewnick, F., Borrmann, S., Weimer, S., Demerjian, K., Salcedo, D., Cottrell, L., Griffin, R., Takami, A., Miyoshi, T.,
- 15 Hatakeyama, S., Shimono, A., Sun, J. Y., Zhang, Y. M., Dzepina, K., Kimmel, J. R., Sueper, D., Jayne, J. T., Herndon, S. C., Trimborn, A. M., Williams, L. R., Wood, E. C., Middlebrook, A. M., Kolb, C. E., Baltensperger, U., and Worsnop, D. R.: Evolution of Organic Aerosols in the Atmosphere, *Science*, 326, 1525–1529, doi:10.1126/science.1180353, 2009.
- Johnson, M. S., Feilberg, K. L., von Hessberg, P., and Nielsen, O. J.: Isotopic processes in atmospheric chemistry, *Chem. Soc. Rev.*, 31, 313–323, doi:10.1039/b108011n, 2002.
- 20 Julien, M., Parinet, J., Nun, P., Bayle, K., Höhener, P., Robins, R. J., and Remaud, G. S.: Fractionation in position-specific isotope composition during vaporization of environmental pollutants measured with isotope ratio monitoring by ¹³C nuclear magnetic resonance spectrometry, *Environ. Pollut.*, 205, 299–306, doi:10.1016/j.envpol.2015.05.047, 2015.
- Kalberer, M., Paulsen, D., Sax, M., Steinbacher, M., Dommen, J., Prevot, A. S. H., Fisseha, R., Weingartner, E., Frankevich, V., Zenobi, R., and Baltensperger, U.: Identification of Polymers as Major Components of Atmospheric Organic Aerosols, *Science*, 303, 1659–1662,
- 25 doi:10.1126/science.1092185, 2004.
- Kalberer, M., Sax, M., and Samburova, V.: Molecular Size Evolution of Oligomers in Organic Aerosols Collected in Urban Atmospheres and Generated in a Smog Chamber, *Environ. Sci. Technol.*, 40, 5917–5922, doi:10.1021/es0525760, 2006.
- Keyword, M. D., Kroll, J. H., Varutbangkul, V., Bahreini, R., Flagan, R. C., and Seinfeld, J. H.: Secondary Organic Aerosol Formation from Cyclohexene Ozonolysis: Effect of OH Scavenger and the Role of Radical Chemistry, *Environ. Sci. Technol.*, 38, 3343–3350,
- 30 doi:10.1021/es049725j, 2004.
- King, S. M., Rosenoern, T., Shilling, J. E., Chen, Q., and Martin, S. T.: Increased cloud activation potential of secondary organic aerosol for atmospheric mass loadings, *Atmos. Chem. Phys.*, 9, 2959–2971, doi:10.5194/acp-9-2959-2009, 2009.

- King, S. M., Butcher, A. C., Rosenørn, T., Coz, E., Lieke, K. I., de Leeuw, G., Nilsson, E. D., and Bilde, M.: Investigating Primary Marine Aerosol Properties: CCN Activity of Sea Salt and Mixed Inorganic–Organic Particles, *Environ. Sci. Technol.*, 46, 10405–10412, doi:10.1021/es300574u, 2012.
- 35 Kirillova, E. N., Andersson, A., Sheesley, R. J., Kruså, M., Praveen, P. S., Budhavant, K., Safai, P. D., Rao, P. S. P., and Gustafsson, O.: ¹³C- and ¹⁴C-based study of sources and atmospheric processing of water-soluble organic carbon (WSOC) in South Asian aerosols, *J. Geophys. Res.-Atmos.*, 118, 614–626, doi:10.1002/jgrd.50130, 2013.
- Kirillova, E. N., Andersson, A., Han, J., Lee, M., and Gustafsson, O.: Sources and light absorption of water-soluble organic carbon aerosols in the outflow from northern China, *Atmos. Chem. Phys.*, 14, 1413–1422, doi:10.5194/acp-14-1413-2014, 2014.
- Kleindienst, T., Smith, D., Li, W., Edney, E., Driscoll, D., Speer, R., and Weathers, W.: Secondary organic aerosol formation from the oxidation of aromatic hydrocarbons in the presence of dry submicron ammonium sulfate aerosol, *Atmos. Environ.*, 33, 3669–3681, doi:10.1016/S1352-2310(99)00121-1, 1999.
- 5 Kristensen, K., Watne, Å. K., Hammes, J., Lutz, A., Petäjä, T., Hallquist, M., Bilde, M. and Glasius, M.: High-Molecular Weight Dimer Esters Are Major Products in Aerosols from α -Pinene Ozonolysis and the Boreal Forest, *Environ. Sci. Technol. Lett.*, doi:10.1021/acs.estlett.6b00152, 2016.
- 10 Kroll, J. H. and Seinfeld, J. H.: Chemistry of secondary organic aerosol: Formation and evolution of low-volatility organics in the atmosphere, *Atmos. Environ.*, 42, 3593–3624, doi:10.1016/j.atmosenv.2008.01.003, 2008.
- Kroll, J. H., Smith, J. D., Che, D. L., Kessler, S. H., Worsnop, D. R., and Wilson, K. R.: Measurement of fragmentation and functionalization pathways in the heterogeneous oxidation of oxidized organic aerosol, *Phys. Chem. Chem. Phys.*, 11, 8005–8014, doi:10.1039/B905289E, 2009.
- 15 Kroll, J. H., Donahue, N. M., Jimenez, J. L., Kessler, S. H., Canagaratna, M. R., Wilson, K. R., Altieri, K. E., Mazzoleni, L. R., Wozniak, A. S., Bluhm, H., Mysak, E. R., Smith, J. D., Kolb, C. E., and Worsnop, D. R.: Carbon oxidation state as a metric for describing the chemistry of atmospheric organic aerosol, *Nat. Chem.*, 3, 133–139, doi:10.1038/nchem.948, 2011.
- Masalaite, A., Remeikis, V., Garbaras, A., Dudoitis, V., Ulevicius, V., and Ceburnis, D.: Elucidating carbonaceous aerosol sources by the stable carbon $\delta^{13}C_{TC}$ ratio in size-segregated particles, *Atmos. Res.*, 158–159, 1–12, doi:10.1016/j.atmosres.2015.01.014, 2015.
- 20 Miyazaki, Y., Fu, P. Q., Kawamura, K., Mizoguchi, Y., and Yamanoi, K.: Seasonal variations of stable carbon isotopic composition and biogenic tracer compounds of water-soluble organic aerosols in a deciduous forest, *Atmos. Chem. Phys.*, 12, 1367–1376, doi:10.5194/acp-12-1367-2012, 2012.
- Narukawa, M., Kawamura, K., Li, S.-M., and Bottenheim, J. W.: Stable carbon isotopic ratios and ionic composition of the high-Arctic aerosols: An increase in $\delta^{13}C$ values from winter to spring, *J. Geophys. Res.-Atmos.*, 113, D02 312, doi:10.1029/2007JD008755, 2008.
- 25 O’Dowd, C., Ceburnis, D., Ovadnevaite, J., Vaishya, A., Rinaldi, M., and Facchini, M. C.: Do anthropogenic, continental or coastal aerosol sources impact on a marine aerosol signature at Mace Head?, *Atmos. Chem. Phys.*, 14, 10 687–10 704, doi:10.5194/acp-14-10687-2014, 2014.
- Pavuluri, C. M., Kawamura, K., Swaminathan, T., and Tachibana, E.: Stable carbon isotopic compositions of total carbon, dicarboxylic acids and glyoxylic acid in the tropical Indian aerosols: Implications for sources and photochemical processing of organic aerosols, *J. Geophys. Res.-Atmos.*, 116, D18 307, doi:10.1029/2011JD015617, 2011.
- 30 Presto, A. A. and Donahue, N. M.: Investigation of alpha-Pinene + Ozone Secondary Organic Aerosol Formation at Low Total Aerosol Mass, *Environ. Sci. Technol.*, 40, 3536–3543, doi:10.1021/es052203z, 2006.

- Rudich, Y., Donahue, N. M., and Mentel, T. F.: Aging of Organic Aerosol: Bridging the Gap Between Laboratory and Field Studies, *Annu. Rev. Phys. Chem.*, 58, 321–352, doi:10.1146/annurev.physchem.58.032806.104432, 2007.
- 35 Rudolph, J. and Czuba, E.: On the use of isotopic composition measurements of volatile organic compounds to determine the “photochemical age” of an air mass, *Geophys. Res. Lett.*, 27, 3865–3868, doi:200010.1029/2000GL011385, 2000.
- Rudolph, J., Czuba, E., and Huang, L.: The stable carbon isotope fractionation for reactions of selected hydrocarbons with OH-radicals and its relevance for atmospheric chemistry, *J. Geophys. Res.*, 105, 29 329–29 346, 2000.
- Sakugawa, H. and Kaplan, I. R.: Stable carbon isotope measurements of atmospheric organic acids in Los Angeles, California, *Geophys. Res. Lett.*, 22, 1509–1512, doi:10.1029/95GL01359, 1995.
- 5 Shilling, J. E., Chen, Q., King, S. M., Rosenørn, T., Kroll, J. H., Worsnop, D. R., McKinney, K. A., and Martin, S. T.: Particle mass yield in secondary organic aerosol formed by the dark ozonolysis of alpha-pinene, *Atmos. Chem. Phys.*, 8, 2073–2088, doi:10.5194/acp-8-2073-2008, 2008.
- Silvestre, V., Mboula, V. M., Jouitteau, C., Akoka, S., Robins, R. J., and Remaud, G. S.: Isotopic ^{13}C NMR spectrometry to assess counterfeiting of active pharmaceutical ingredients: Site-specific ^{13}C content of aspirin and paracetamol, *J. Pharmaceut. Biomed.*, 50, 336–341, doi:10.1016/j.jpba.2009.04.030, 2009.
- 10 Stocker, T. F., Qin, D., Plattner, G.-K., Tignor, M., Allen, S. K., Boschung, J., Nauels, A., Xia, Y., Bex, V., and Midgley, P., eds.: IPCC, 2013: Climate Change 2013: The Physical Science Basis. Contribution of Working Group I to the Fifth Assessment Report of the Intergovernmental Panel on Climate Change, Cambridge University Press, Cambridge, United Kingdom and New York, NY, USA, 2013.
- Subramanian, R., Khlystov, A. Y., Cabada, J. C., and Robinson, A. L.: Positive and Negative Artifacts in Particulate Organic Carbon Measurements with Denuded and Undenuded Sampler Configurations, *Aerosol Sci. Tech.*, 38, 27–48, doi:10.1080/02786820390229354, 2004.
- 15 Timkovsky, J., Dusek, U., Henzing, J. S., Kuipers, T. L., Röckmann, T., and Holzinger, R.: Offline thermal-desorption proton-transfer-reaction mass spectrometry to study composition of organic aerosol, *J. Aerosol Sci.*, 79, 1–14, doi:10.1016/j.jaerosci.2014.08.010, 2015.
- Tolocka, M. P., Jang, M., Ginter, J. M., Cox, F. J., Kamens, R. M., and Johnston, M. V.: Formation of Oligomers in Secondary Organic Aerosol, *Environ. Sci. Technol.*, 38, 1428–1434, doi:10.1021/es035030r, 2004.
- 20 Turekian, V. C., Macko, S. A., and Keene, W. C.: Concentrations, isotopic compositions, and sources of size-resolved, particulate organic carbon and oxalate in near-surface marine air at Bermuda during spring, *J. Geophys. Res.*, 108, 4157, doi:10.1029/2002JD002053, 2003.
- Turpin, B. J., Saxena, P., and Andrews, E.: Measuring and simulating particulate organics in the atmosphere: problems and prospects, *Atmos. Environ.*, 34, 2983–3013, 2000.
- Wade, D.: Deuterium isotope effects on noncovalent interactions between molecules, *Chemico-Biological Interactions*, 117, 191–217, doi:10.1016/S0009-2797(98)00097-0, 1999.
- 25 Watson, J. G., Chow, J. C., Chen, L.-W. A., and Frank, N. H.: Methods to Assess Carbonaceous Aerosol Sampling Artifacts for IMPROVE and Other Long-Term Networks, *J. Air Waste Manage.*, 59, 898–911, doi:10.3155/1047-3289.59.8.898, 2009.
- Werner, R. A. and Brand, W. A.: Referencing strategies and techniques in stable isotope ratio analysis, *Rapid Commun. Mass Sp.*, 15, 501–519, doi:10.1002/rcm.258, 2001.
- 30 Werner, R. A., Bruch, B. A., and Brand, W. A.: ConFlo III – an interface for high precision d^{13}C and d^{15}N analysis with an extended dynamic range, *Rapid Commun. Mass Sp.*, 13, 1237–1241, doi:10.1002/(SICI)1097-0231(19990715)13:13<1237::AID-RCM633>3.0.CO;2-C, 1999.
- Widory, D., Roy, S., Le Moullec, Y., Goupil, G., Cocherie, A., and Guerrot, C.: The origin of atmospheric particles in Paris: a view through carbon and lead isotopes, *Atmos. Environ.*, 38, 953–961, doi:10.1016/j.atmosenv.2003.11.001, 2004.

- 35 Williams, E. L. and Grosjean, D.: Removal of atmospheric oxidants with annular denuders, *Environ. Sci. Technol.*, 24, 811–814, doi:10.1021/es00076a002, 1990.
- Winterhalter, R., Van Dingenen, R., Larsen, B. R., Jensen, N. R., and Hjorth, J.: LC-MS analysis of aerosol particles from the oxidation of alpha-pinene by ozone and OH-radicals, *Atmos. Chem. Phys. Discuss.*, 3, 1–39, doi:10.5194/acpd-3-1-2003, 2003.
- Witter, M., Berndt, T., Böge, O., Stratmann, F., and Heintzenberg, J.: Gas-phase ozonolysis: Rate coefficients for a series of terpenes and rate coefficients and OH yields for 2-methyl-2-butene and 2,3-dimethyl-2-butene, *Int. J. Chem. Kinet.*, 34, 394–403, doi:10.1002/kin.10063, 2002.

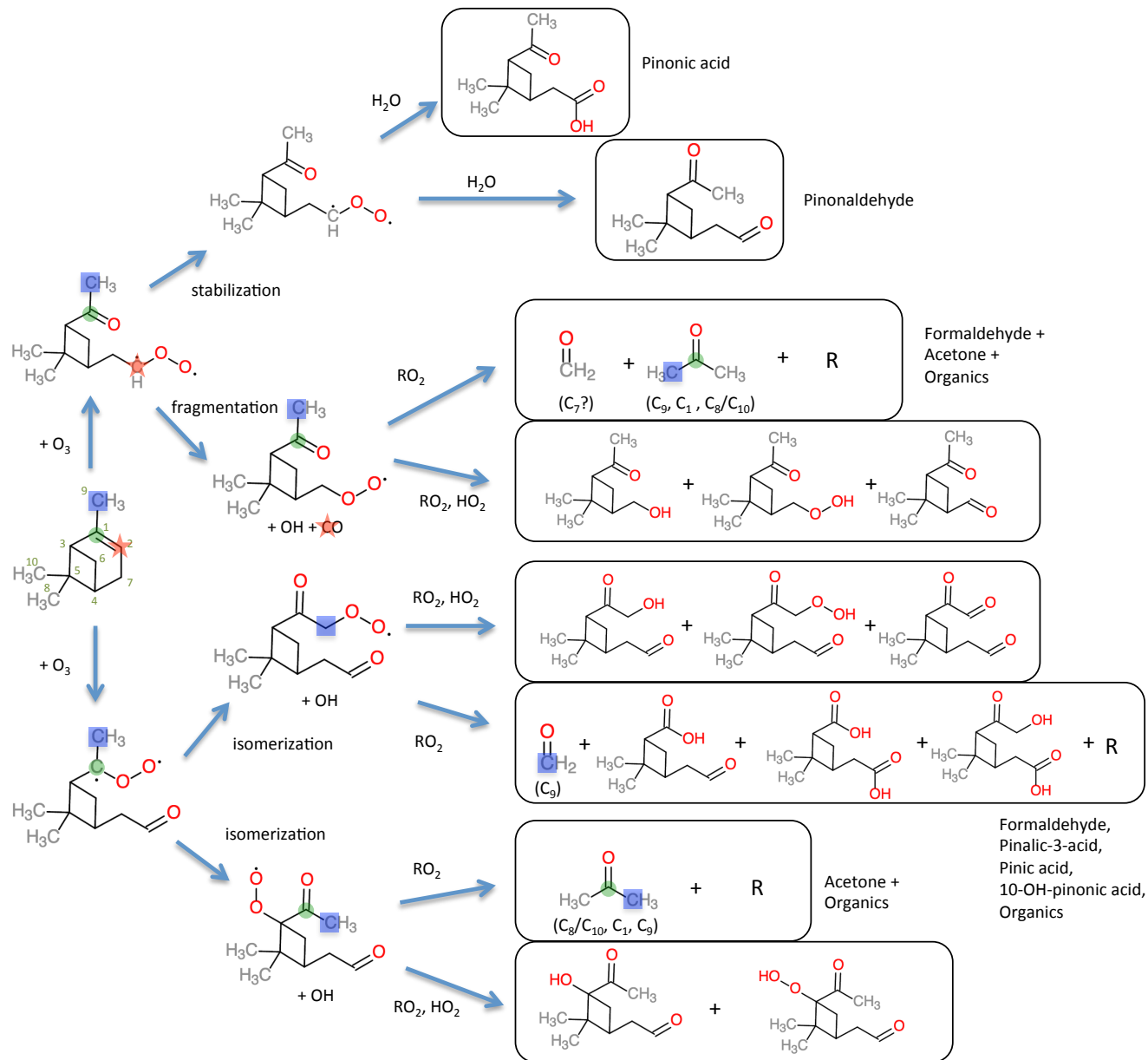


Figure 1. Reaction scheme of α -pinene ozonolysis, based on Camredon et al. (2010), using the reaction mechanism of MCMv3.1. The boxes show first-generation products while subsequent dimer formation and oligomerization are not shown. The O:C ratio typically increases as oxidation proceeds (i.e. oxygen addition via functionalization). Large, oxygenated product compounds (e.g. pinonic acid, pinonaldehyde) have lower vapour pressures and partition to the particle phase. Small, volatile products including HCHO, acetone and CO result from fragmentation processes and partition to the gas phase. The coloured symbols highlight how the parent α -pinene's atoms (denoted in brackets) can form small reaction products including CO, HCHO and acetone. The symbol colours were chosen based on the heat map in Fig. 7.

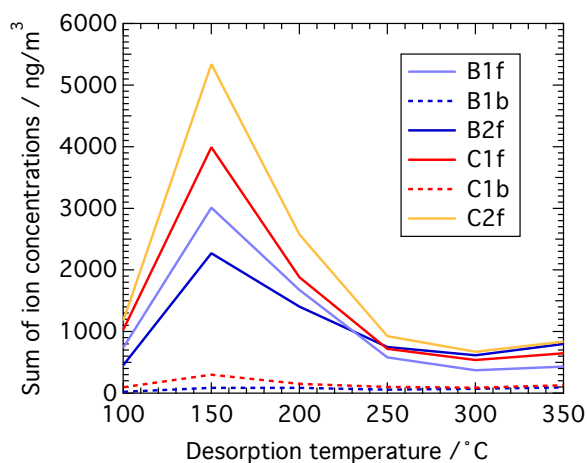


Figure 2. Sum of ion concentrations of desorbed SOA filter material from α -pinene ozonolysis as detected by PTR-MS. The concentrations of all detected ions were summed for each desorption temperature. [..¹⁹⁵] Full lines represent front filters, dashed lines back filters. [..¹⁹⁶]

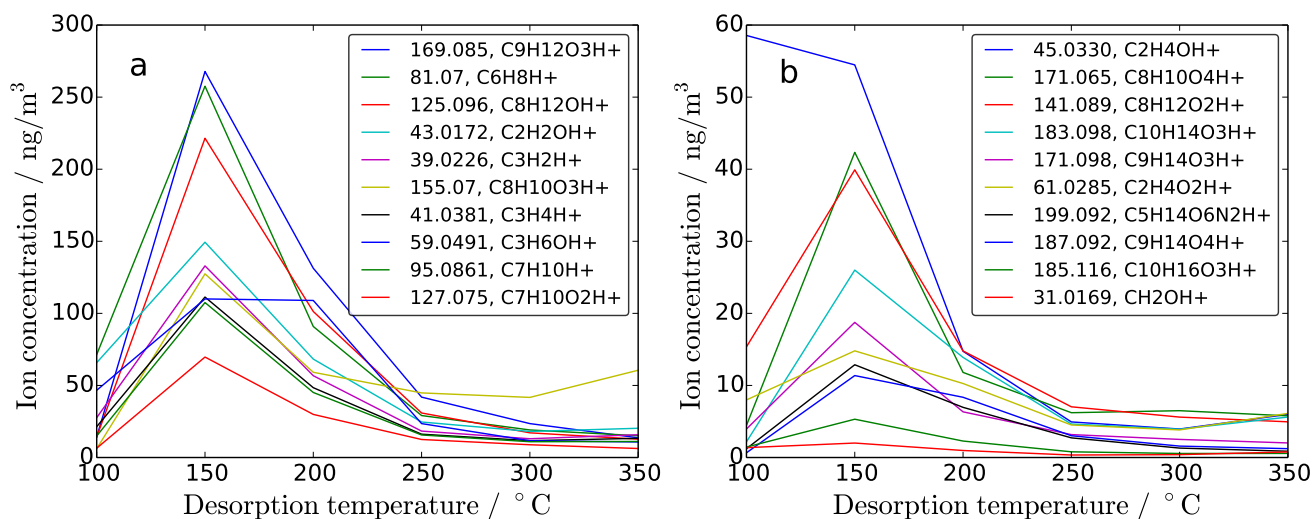


Figure 3. Ion concentration thermograms of compounds desorbing from filter C1f as detected by PTR-MS. Filter C1f contains SOA from α -pinene ozonolysis in dark and dry conditions using cyclohexane as an OH scavenger. All ions are labeled by their masses in Da and their identified molecular formula. Ions with the largest concentrations are listed first. The ten ions with highest mass concentrations are plotted in Panel a. The most abundant ions found in this study with masses similar to compounds reported in the literature [..¹⁹⁷] (see Table 3) are plotted in Panel b. These are the same compounds as below the line in Table 4 and include those predicted by the MCM, e.g. pinic acid (187.093 Da) and pinonic acid (185.117 Da). See Sect. S4 [..¹⁹⁸] for more details. Most ions show a peak at 150 °C, but their desorption patterns differ at lower and higher temperatures.

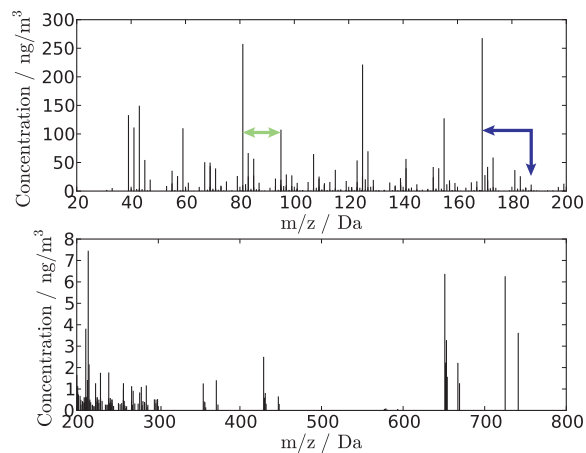


Figure 4. Mass spectrum of SOA from the dark ozonolysis of α -pinene (using cyclohexane as OH scavenger) desorbed from filter C1f at 150 °C (note the difference in scale between the two panels). The presence of lobes with specific periodicity is apparent. The arrows highlight two detected fragmentation patterns that cause the periodicity: that of a CH_2 group (light green arrow) and that of water (dark blue arrow), cf. Sect. S4[..¹⁹⁹].

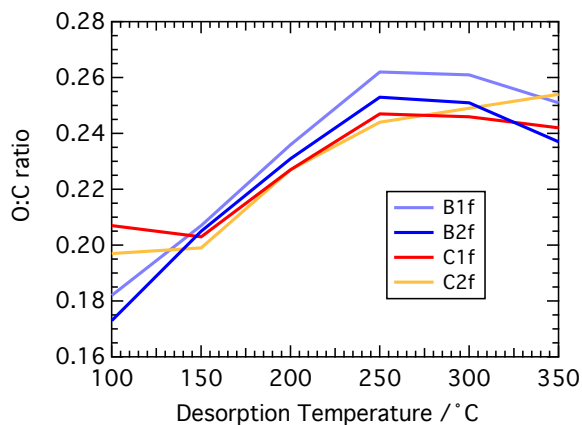


Figure 5. Measured oxygen to carbon ratios (O:C) of α -pinene SOA desorbing from filters at different temperatures.[..²⁰⁰]

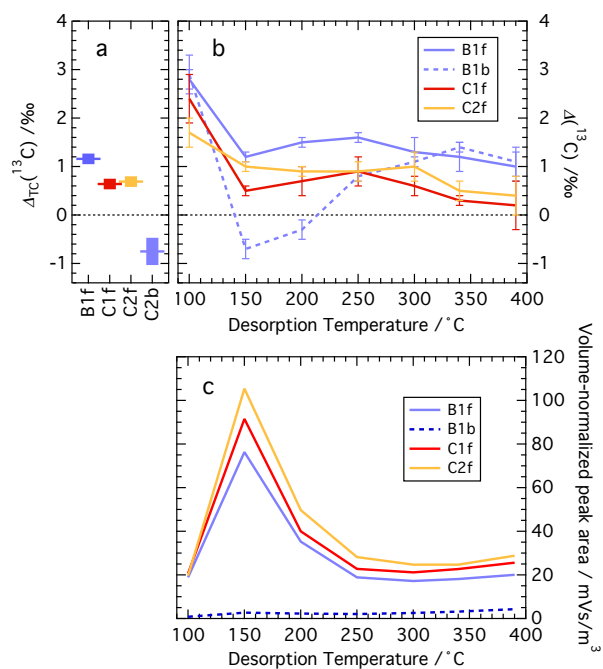


Figure 6. $\Delta(^{13}\text{C})$ values of alpha-pinene SOA filter samples and corresponding peak areas. [..²⁰¹] Full lines represent front filters, and dashed lines back filters. Error bars denote 1- σ standard deviations and are propagated; they vary with loading. Panel a: TC analysis of selected filters (see x-axis). Panel b: Thermal desorption analysis of filter material. Panel c: Volume-normalized (not blank corrected) peak area as function of desorption temperature for the same data as in Panel b.

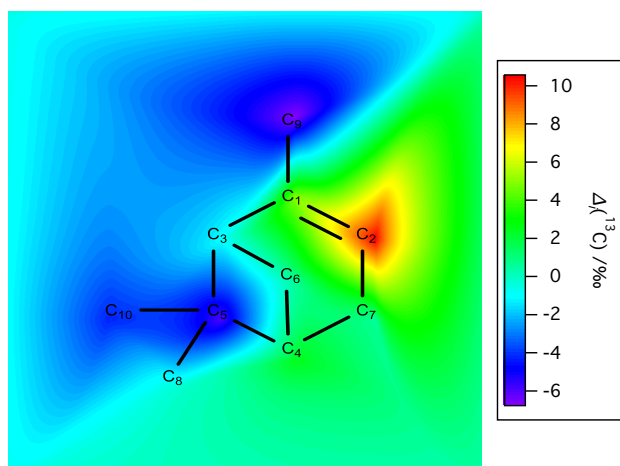


Figure 7. Heat map of $\Delta_i(^{13}\text{C})$ in α -pinene (Sigma-Aldrich, lot MKBQ6213V) relative to its bulk isotopic composition, cf. Table 1. The boundary of the image was set to $\Delta_i(^{13}\text{C}) = 0$, i.e. the bulk isotopic composition. A large enrichment is visible at the double bond (C₂), and large depletions are visible at positions C₅ and C₉ where isotopic substitution is expected to reduce the molar volume significantly. C-atoms are numbered in order of decreasing ^{13}C chemical shifts in the ^{13}C NMR spectrum.

Table 1. Manufacturer information and isotopic composition of α -pinene samples. Position-specific isotopic fractionation is given as isotopic difference, $\Delta_i(^{13}\text{C}) = \delta_i(^{13}\text{C}) - \delta_{\text{TC}}^{\circ j}(^{13}\text{C})$ of individual C-atoms (i) in α -pinene sample j with bulk isotopic composition $\delta_{\text{TC}}^{\circ j}(^{13}\text{C})$. Listed are the means of 5 measurements. See inserted figure for numbering of C-atoms. Sample 1 was used in the chamber experiments, but PSIA could not be performed as no more sample was available.

| Sample j | Manufacturer | Purity /% | Code | Lot | $\delta_{\text{TC}}^{\circ j}(^{13}\text{C})$ /‰ | $\Delta_i(^{13}\text{C})$ / ‰ | | | | | | | | | | |
|------------|----------------|--------------|-----------|------------|---|-------------------------------|----------------|----------------|----------------|----------------|------------------|----------------|----------------|-----------------|--|--|
| | | | | | | C ₁ | C ₂ | C ₃ | C ₄ | C ₅ | C _{6,7} | C ₈ | C ₉ | C ₁₀ | | |
| 1 | Sigma-Aldrich | >99 | 268070 | 80796DJV | -30.0 | | | | | | | | | | | |
| 2 | Sigma-Aldrich | >99 | 268070 | MKBQ6213V | -27.7 | 4.8 | 10.5 | -1.0 | 2.4 | -6.0 | 0.6 | -0.3 | -6.7 | -4.3 | | |
| 3 | Acros Organics | 98 | 131261000 | A0310018 | -27.0 | 4.1 | 10.4 | -1.3 | 3.2 | -5.2 | 1.9 | -0.2 | -6.9 | -5.4 | | |
| 4 | Merck | >97 | 818632 | S21251 423 | -28.1 | 6.1 | 9.6 | -1.4 | 3.6 | -3.8 | -0.8 | -1.2 | -5.2 | -3.9 | | |
| 5 | Alfa Aesar | 98 | L04941 | 10175835 | -27.8 | 7.8 | 5.8 | -0.8 | 4.2 | 0.0 | -1.8 | -3.6 | -4.5 | -3.3 | | |

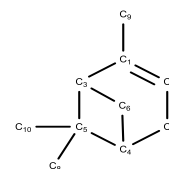


Table 2. Overview of α -pinene ($\delta_{\text{TC}}^{\text{O}1}(^{13}\text{C}) = (-29.96 \pm 0.08) \text{‰}$) ozonolysis experiments using 1-butanol (B) or cyclohexane (C) as OH-scavenger. Filter ID's are [..²⁰²] explained in the [..²⁰³]text. The sampling time, t , and the sampled volume, V , are given. Isotopic data at 100 °C and 150 °C and for total carbon (TC) is given as $\Delta(^{13}\text{C}) = \delta(^{13}\text{C}) - \delta_{\text{TC}}^{\text{O}1}(^{13}\text{C})$. The total aerosol mass loading as detected by PTR-MS, $M_{\text{total}}^{\text{PTR-MS}}$, is listed next. The last column lists the measured O:C ratio averaged over all desorption temperatures.

| Experiment | Filter ID | t / h [.. ²⁰⁴] | V / m^3 [.. ²⁰⁵] | $\Delta(^{13}\text{C}) / \text{‰}$ | | | $M_{\text{total}}^{\text{PTR-MS}} / \mu\text{g}/\text{m}^3$ | O:C |
|---|-----------|-------------------------------------|---------------------------------------|------------------------------------|----------|----------|---|------|
| | | | | 100 °C | 150 °C | TC | | |
| B ^a (α -pinene, 1-butanol) | B1f | 47 [.. ²⁰⁶] | 28.2 [.. ²⁰⁷] | 2.8±0.2 | 1.2±0.1 | 1.2±.1 | 6.9 | 0.23 |
| | B1b | 47 [.. ²⁰⁸] | 28.2 [.. ²⁰⁹] | 2.9±0.4 | -0.7±0.2 | – | 0.4 | 0.21 |
| | B2f | 16.8 [.. ²¹⁰] | 10.1 [.. ²¹¹] | – | – | – | 6.3 | 0.22 |
| | B2b | 16.8 [.. ²¹²] | 10.1 [.. ²¹³] | – | – | – | – | – |
| C (α -pinene, cyclohexane) | C1f | 24.5 [.. ²¹⁴] | 14.7 | 2.4±0.5 | 0.5±0.1 | 0.6±0.1 | 8.9 | 0.23 |
| | C1b | 24.5 [.. ²¹⁵] | 14.7 [.. ²¹⁶] | – | – | – | 0.9 | 0.22 |
| | C2f | 26.7 [.. ²¹⁷] | 16.5 [.. ²¹⁸] | 1.7±0.3 | 1.0±0.1 | 0.7±0.1 | 11.7 | 0.23 |
| | C2b | 26.7 [.. ²¹⁹] | 16.5 [.. ²²⁰] | – | – | -0.8±0.3 | – | – |
| Handling blank | HB | – | – | 10.0±0.8 | 8.9±0.1 | – | 0.23 ^b | – |

^a CCN data available, see Sect. S2[..²²¹]

^b Surface loading in units of $\mu\text{g}/\text{cm}^2$

Table 3. Main references cited in this study for comparison of chemical composition. The identifier (last column) denotes the letter the reference corresponds to in Table 4 and Sect. S6[..²²²]. Abbreviations: [..²²³]QP: Quadrupole, TD: Thermal-desorption, TOF: Time-of-Flight, [..²²⁴]LC: Liquid-Chromatography[..²²⁵], [..²²⁶]MS: [..²²⁷]Mass-Spectrometer, [..²²⁸]GC: [..²²⁹]Gas-Chromatography, [..²³⁰]HP: [..²³¹]High-Performance.

| Study | Sample | Sample phase | Instrumentation / method | Identifier |
|----------------------------|---|---------------|--------------------------|------------|
| Holzinger et al. (2005) | Ambient, forest | Gas | PTR-MS (QP) | - |
| Holzinger et al. (2010a) | Ambient, Austrian alps | Aerosol | TD-PTR-MS (TOF) | a |
| Winterhalter et al. (2003) | α -pinene ozonolysis | Aerosol | LC-MS | b |
| Jaoui and Kamens (2003) | α -pinene + β -pinene ozonolysis | Aerosol | GC-MS, HP-LC | c |
| Jenkin (2004) | α -pinene ozonolysis | Gas + aerosol | Modelling | d |
| Camredon et al. (2010) | α -pinene ozonolysis | Gas + aerosol | MCM Modelling | * |

* MCM names

Table 4. The 20 ions with the highest concentrations [..²³²] from [..²³³] filter C1f at 150 °C, plus ten ions with nominal masses similar to protonated compounds commonly reported in the literature (below the line). Ions are sorted by their measured mass (m/z). [..²³⁴] The chemical formula and [..²³⁵] concentration, w [..²³⁶], are shown for each ion, and in parenthesis, its ranking out of the 451 [..²³⁷] ions. The concentration ratio between back filter C1b and the corresponding front filter (C1f) at 150 °C is calculated for each listed compound [..²³⁸]. [..²³⁹] Assignments in the [..²⁴⁰] literature which seem to be in [..²⁴¹] error are indicated by parenthesis. [..²⁴²] Ions that are part of the same sequence of the H₂O-loss fragmentation pattern (cf. Sect. S4 [..²⁴³] for definition) are numbered relative to each other as $\pm n \times 18.011$ Da ($\pm n$ and the compound's ranking are given). Here a dash means that the peak was identified but not resolved. The list of all ions detected from compounds desorbing from filter 6 can be found in Sect. S6 [..²⁴⁴].

| Mass/Da | Formula | w / ng/m ³ (Rank) | Back / Front | Description | Literature | H ₂ O number n (Rank) |
|---------|------------|--------------------------------|--------------|---|--------------|------------------------------------|
| 39.0226 | C3H2H+ | 132.93 (5) | 0.03 | | | |
| 41.0381 | C3H4H+ | 111.32 (7) | 0.03 | | | |
| 43.0172 | C2H2OH+ | 149.37 (4) | 0.05 | | a | |
| 45.033 | C2H4OH+ | 54.47 (16) | 0.01 | Acetaldehyde | a | +1 (336) |
| 59.0491 | C3H6OH+ | 110.01 (8) | 0.06 | Acetone | a, c | |
| 67.0546 | C5H6H+ | 50.57 (18) | 0.04 | | | |
| 69.0337 | C4H4OH+ | 49.81 (19) | 0.01 | | | |
| 69.0699 | C5H8H+ | 43.60 (20) | 0.03 | | | |
| 81.07 | C6H8H+ | 257.57 (2) | 0.03 | Similar to #9 | | +1 (32) |
| 83.0496 | C5H6OH+ | 66.57 (11) | 0.05 | | a | +1 (62), -1 (96) |
| 85.065 | C5H8OH+ | 56.71 (14) | 0.01 | | | |
| 95.0861 | C7H10H+ | 107.50 (9) | 0.03 | Similar to #2 | | |
| 107.086 | C8H10H+ | 64.79 (12) | 0.19 | | | |
| 123.081 | C8H10OH+ | 53.69 (17) | 0.02 | | a | -1 (58) |
| 125.096 | C8H12OH+ | 221.48 (3) | 0.02 | | | |
| 127.075 | C7H10O2H+ | 69.69 (10) | 0.01 | | | |
| 141.054 | C7H8O3H+ | 56.22 (15) | 0.17 | | a | +1 (63) |
| 155.07 | C8H10O3H+ | 127.41 (6) | 0.01 | | a, (b, d) | +1 (13) |
| 169.085 | C9H12O3H+ | 267.79 (1) | 0.01 | | (c, d), a | +1 (72), -1 (22), -2 (202) |
| 173.079 | C8H12O4H+ | 58.75 (13) | 0.01 | Norpinonic acid | b, d, (b) | -1 (6) |
| 31.017 | CH2OH+ | 2.01 (179) | 0.07 | Formaldehyde | a, c, d | |
| 61.0286 | C2H4O2H+ | 14.80 (59) | 0.06 | Acetic acid | a | |
| 141.089 | C8H12O2H+ | 39.91 (24) | 0.03 | 2,2-Dimethyl-cyclobutyl-1,3-diethanal | a, d, (d) | |
| 171.065 | C8H10O4H+ | 42.34 (21) | 0.03 | not norpinonic acid | a, (b, c, d) | -1 (-) |
| 171.098 | C9H14O3H+ | 18.75 (48) | 0.07 | norpinonic acid (?) | b, c, d | |
| 183.099 | C10H14O3H+ | 26.00 (35) | 0.03 | C109CO, 4-Oxopinonaldehyde | b, c, d | +1 (232), +2 (-) |
| 185.117 | C10H16O3H+ | 5.31 (114) | 0.12 | pinonic acid, OH-pinonaldehyde, PINONIC, C107OH, C109OH | (a), b, c, d | -1 (51), -2 (132) |
| 187.093 | C9H14O4H+ | 11.37 (71) | 0.01 | pinic acid, 10-OH norpinonic acid, PINIC | b, (b), c, d | -1 (1), -2 (22), -3 (200) |
| 199.093 | C10H14O4H+ | 12.87 (66) | 0.01 | oxopinonic acid, keto-pinonic acid | b, d | -1 (27), -2 (105), +1 (380) |

^a Holzinger et al. (2010a), ^b Winterhalter et al. (2003), ^c Jenkin (2004), ^d Jaoui and Kamens (2003)

Table 5. Calculated $\Delta(^{13}\text{C})$ values assuming that fragmentation yields certain C-atoms to be expelled to the gas phase and others to partition to the aerosol phase (details in Sect. 3.3.2). Calculations based on position-specific measurement results of the Sigma-Aldrich sample in Table 1. See Fig. 7 for numbering of C-atoms.

| Expelled C-atom(s) | $\Delta_{\text{gas}}(^{13}\text{C})$ /‰ | $\Delta_{\text{aerosol}}(^{13}\text{C})$ /‰ |
|---|---|---|
| C ₁ | 4.9 | -0.4 |
| C ₂ | 10.5 | -1.1 |
| C ₇ | 0.6 | 0.0 |
| C ₉ | -6.7 | 0.8 |
| C ₈ + C ₁ + C ₉ | -0.7 | 0.4 |
| C ₁₀ + C ₁ + C ₉ | -2.0 | 1.0 |